CNN Filter DB: An Empirical Investigation of Trained Convolutional Filters

Supplementary Material

A. Dataset details

We provide *CNN Filter DB* as a ca. 100 GB large HDF5 file which contains the unprocessed 3×3 filters along with meta information as reported in Tab. 3.

We have collected models of the following tasks: *Classification, GAN-Generator, Segmentation, Object Detection, Style Transfer, Depth Estimation, Face Detection, Super Resolution, GAN-Discriminator, Face Recognition, Auto-Encoder*. The training sets were distributed into the following categories: *plants, natural, art, map, handwriting, medical ct, medical mri, depth, faces, textures, fractals, seismic, astronomy, thermal, medical xray, cars*.

A visualization of the accumulated frequency of models and filters by task, visual category, and training dataset combination can be found in Fig. 17. Heatmaps for aggregated frequency of filters/models by task and visual category are shown in Fig. 1.

As previously mentioned, we used rescaled filters for all distribution shift related experiments. In Fig. 2 we show the mean scale per layer depth decile of the unprocessed filters. We group the filters f by model and depth decile in sets S and compute the mean scale as follows:

$$\hat{scale} = \sum_{f \in S} \frac{\max_{ij} f_{ij} - \min_{ij} f_{ij}}{|S|} \tag{1}$$

The distributions show an unsurprising decrease with depth but also a high variance and many outliers across models, especially in the first two deciles.

Lastly, Tab. 4 contains all models we have used for our analysis.

B. Derivation of randomness threshold

We draw $n = 2^1, \ldots, 2^{21}$ filters with 3×3 shape from a standard normal distribution and calculate the entropy H as defined in the *Methods* section. We repeat this process 1000 times for each n and fit a sigmoid to the lowest entropy we have observed for each n. Fig. 3 shows the obtained samples alongside the fitted sigmoid T_H.

C. Ablation study: Degeneration impact

As mentioned in the *Limitations* section, we attempted to reproduce our experiments with a dataset that did not include filters from degenerated layers. We applied the following selection criterion to detect degeneration based on entropy H and sparsity S as defined in our *Methods* section:

$$(H \geq T_H - 0.02) \vee (H < 0.5) \wedge (S \geq 0.14) \tag{2}$$

While we had a solid foundation for the entropy upper bound (minus some noise), the lower bound for entropy and the bound for sparsity are based on the average we found in our datasets. Note that increasing the lower bound for H results in more similar distributions and therefore lower shift. Hence, this value should be picked very carefully to not filter out vital layers. Sparsity is usually seen in peaks around the center of the KDEs. Tuning this value has a significant impact on the shift (Fig. 6) since the large center peaks increase the KL-Divergence significantly (Fig. 4). With the selected threshold we fail to find a meaningful correlation between the ratio of degenerated layers and the average shift to other groups (i.e. *tasks* or *visual categories*; Fig. 5).

D. Distribution shift by precision

We initially assumed that quantization may lead to the *spikes* phenotype, so we decided to test what shift we obtain when training with fp16 instead of fp32 precision. Spiky distributions should show high shifts in comparison to smooth distributions. We train all our low resolution models on *CIFAR-10* with the same hyperparameters and observe marginal shifts Fig. 7. Outliers with somewhat higher shifts include *MobileNet_v2*. But we have verified that the shift for *MobileNet_v2* does not exceed the shift one would measure by retraining with random seeds. The *ResNet-9* shift does not exceed its retraining shift, therefore we assume that this also applies to other models.

E. Distribution shift by convolution depth

In addition to the main paper we also report the shift by absolute depth for the first 20 layers in Fig. 8 of *classification* models and the shift by relative depth for more tasks in Fig. 9. Please note, that Fig. 9e only contains the same network trained on different datasets.

F. More principal components

In Fig. 10 we add interesting counter-parts to the filter basis shown in the main paper. As one can observe the filter basis remains quite similar. Changes usually affect the order of the components (since they are sorted by explained variance ratio), inversion (though this is not characteristic, since the coefficients can simply be inverted), and noise presumably due to degeneration. Fig. 11 contains the

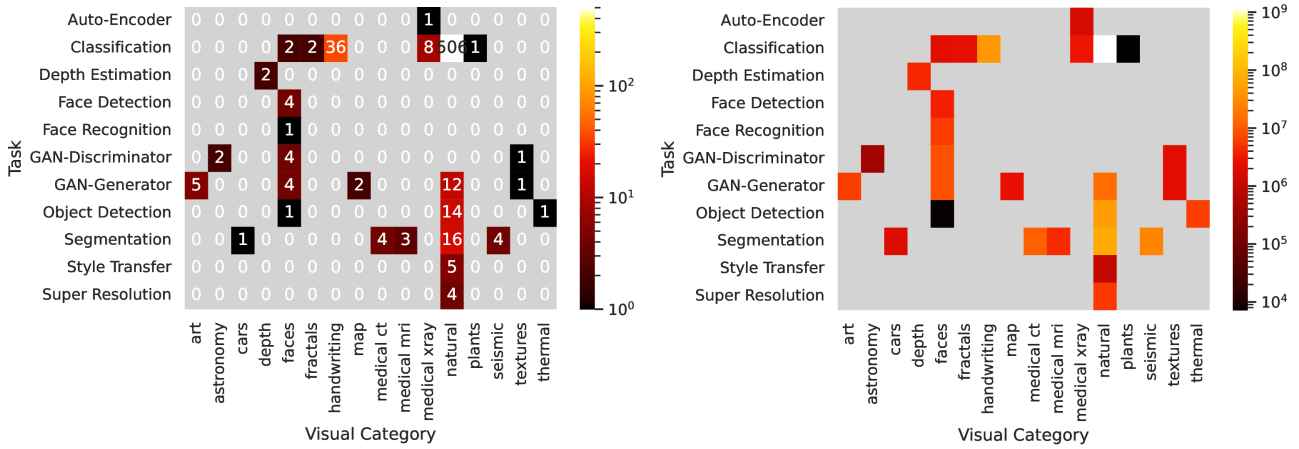

(a) model frequency

(b) filter frequency

Figure 1. Bi-variate heatmap showing frequency aggregated by task and visual category.

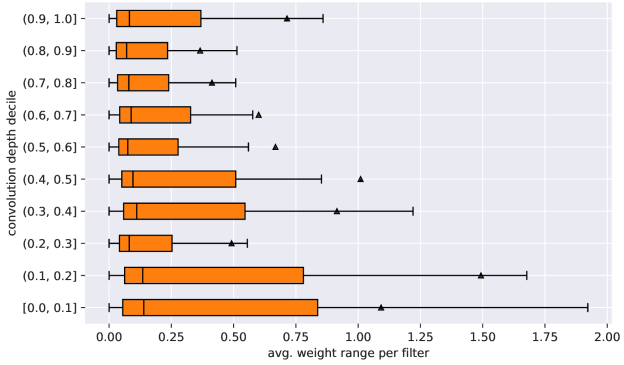

Figure 2. Boxplots showing average filter range per convolution depth decile (top to bottom in decreasing order) for each classification model in the dataset. Outliers are hidden for clarity.

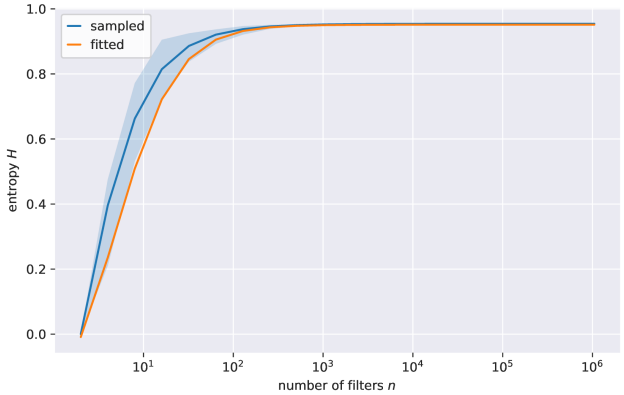

Figure 3. Sampled entropy for randomly initialized convolution layers with n filters and fitted sigmoid T_H.

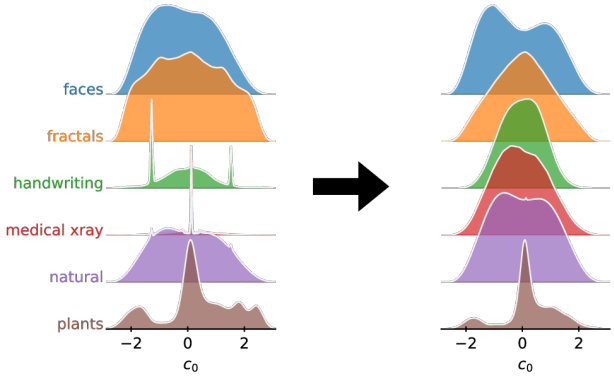

Figure 4. Most significant principal component KDEs of classification models by tasks before (left) and after removal of degenerated layers (right).

cumulative explained variance ratio plots for all tasks and visual categories. For the sake of completeness, we also add that SVD centering $\bar{X} = [-0.04262863, -0.0411367, -0.04461834, -0.0407119, -0.03574134, -0.04268694, -0.04350573, -0.04138637, -0.04486743]$ for the full dataset.

G. More KDEs plots

Fig. 18 shows the KDEs (KDEs created with [1]) for every principal component on the full dataset. Fig. 19 shows KDEs for all tasks. Fig. 21 shows only KDEs of tasks of models that were trained with datasets belonging to the natural visual category. Fig. 20 shows KDEs for every visual category. Some categories show shifts due to bias representation while other clearly contain a majority of degenerated filters. Fig. 22 show KDEs by the visual category of

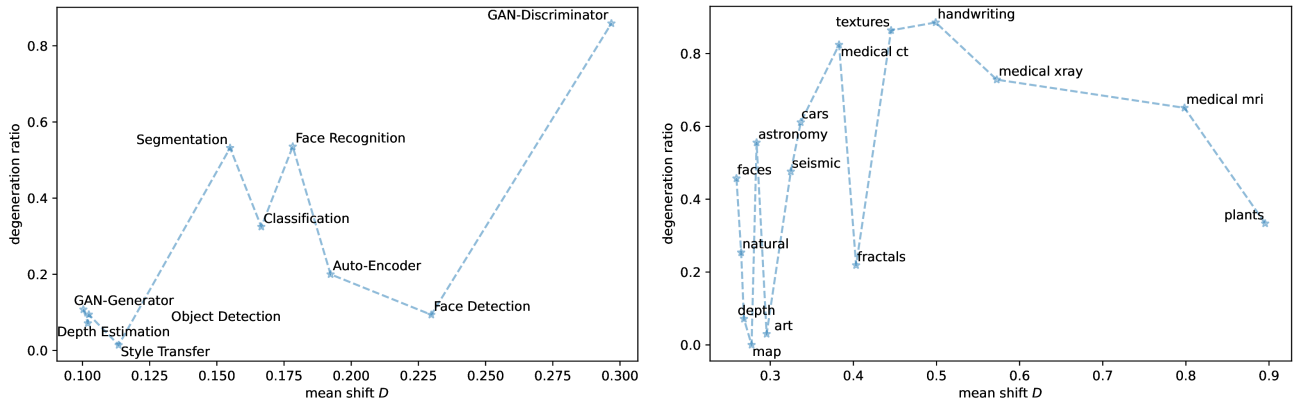

(a) tasks (b) visual category

Figure 5. (Lack of) correlation between mean shift D and layer degeneration ratio.

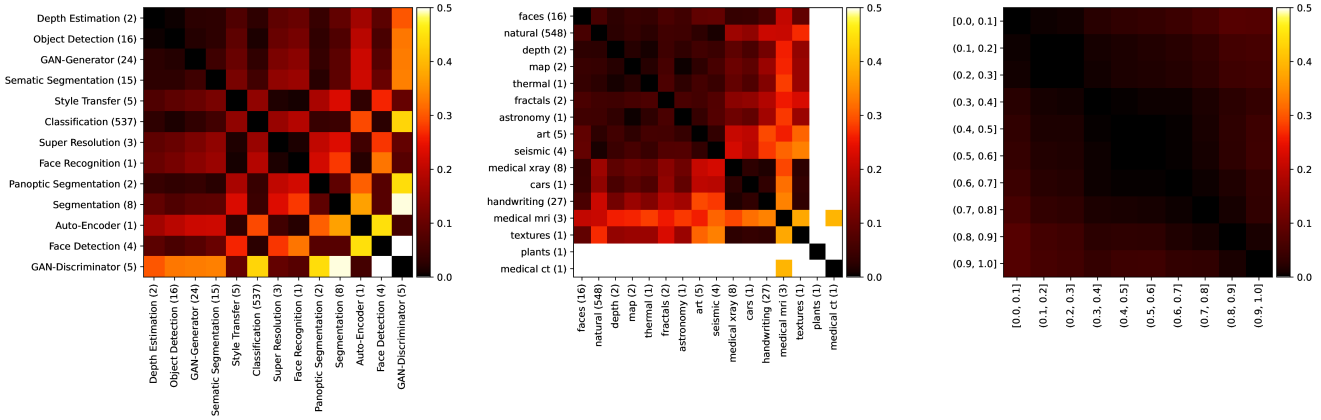

(a) tasks (b) visual categories (c) convolution depth decile

Figure 6. Heatmaps over the shift D for different filters groupings computed on the dataset *without degenerated layers*. The number in brackets denotes the number of models in this group. Low values/dark colors denote low shifts.

the training dataset limited to classification models. Several categories such as *medical xray, plants, handwriting* are clearly impacted by degeneration. Fig. 23 shows KDEs of classification models split by convolution depth decile. The distribution shift with depth reminds us of the shift of all filters we have seen during training *ResNet-9* in our *Results* section. Fig. 25 shows some selected models from the same family, showing clear shifts between the families but low shifts within. Lastly, Fig. 24 shows all models trained on *MNIST*. These are consist exclusively of the intentionally overparameterized models. The KDEs show very clear signs of major degeneration, by stark spikes, especially around null.

H. Phenotype scatter plots

The main paper showed only scatter plots between two select coefficient distributions c_i and c_j. Here we include the all bi-variate scatter plots of selected examples for each phenotype over all pairs of distributions (i.e. $i = 0, \ldots, 8$ and $j = 0, \ldots, 8$):

Fig. 12 shows the scatter plots over all filters that we have extracted;Fig. 13 shows *spikes* of filters that belong to the visual category *medical ct*; Fig. 14 shows *symbols* based on filters that belong to an *EfficientNet-l2-ns-475* pretrained on the massive *JFT-300m* and fintetuned on *ImageNet1k*; Fig. 15 shows *point* computed on filters of our intentionally overparameterized models trained on *MNIST*; and Fig. 16 shows *spikes* computed on filters of the task *depth estimation*.

I. Training of low resolution models

Models were taken from [2] and slightly modified by us to support different input channel and class modalities. Additionally, some more architectures were added. Generally,

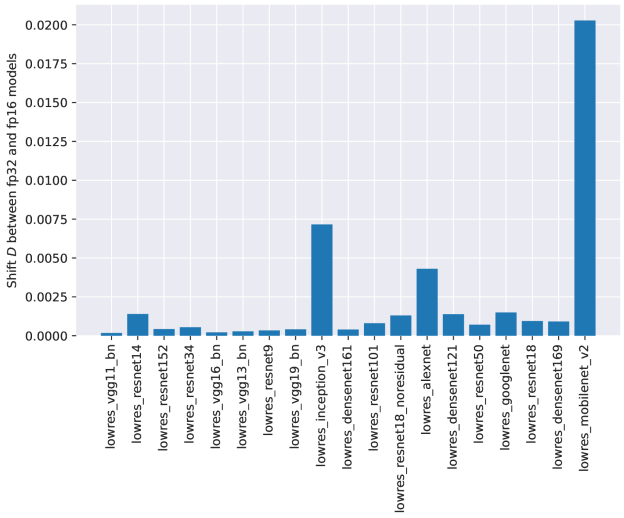

Figure 7. Distribution shift D between low resolution models between trained on *CIFAR-10* with fp16 and fp32 precision.

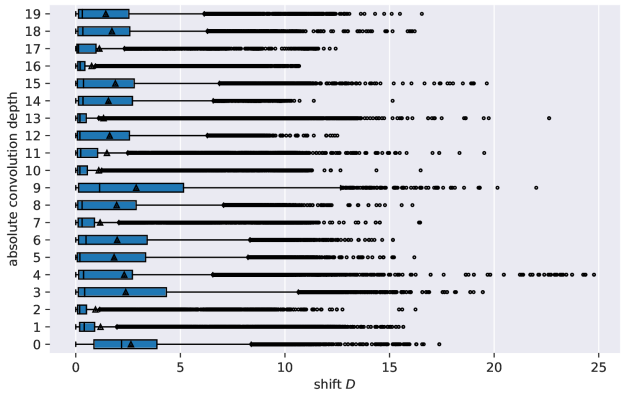

Figure 8. Boxplots showing the distribution of pair-wise model-to-model shift D of *classification* models per convolution depth. Our intentionally overparameterized models were left out of this analysis.

these models are quite similar to the architectures proposed in their respective original publications. However typically, Pooling will be reduced, dilated or strided convolutions will be replaced by regular convolutions, and convolution kernel sizes are reduced to be no larger than 3×3.

All models are trained on NVIDIA A100 GPUs and hyper-parameters independent of the dataset. Stochastic matrix multiplication is turned off via cuDNN settings. Inputs are scaled to 32×32 px and channel-wise normalized. CIFAR data is additionally zero-padded by 4 px along each dimension, and then transformed using a 32×32 random crops, and random horizontal flips. For the hyper parameters an initial learning rate of 1e-8, a weight decay of 1e-2, a batch-size of 256 and a nesterov momentum of 0.9 is used.

Table 1. Performance of retrained ResNet-9 models with random seeds obtained after the validation epoch with the highest validation accuracy.

Model ID	Best Epoch	Train Loss	Train Accur.	Valid. Loss	Valid. Accur.
resnet9_0	93	0.016	99.996	0.174	94.792
resnet9_1	94	0.016	99.980	0.176	94.631
resnet9_2	96	0.016	99.986	0.177	94.571
resnet9_3	89	0.017	99.976	0.175	94.812
resnet9_4	99	0.015	99.992	0.175	94.762
resnet9_5	94	0.016	99.994	0.174	94.822
resnet9_6	91	0.016	99.986	0.175	94.812
resnet9_7	94	0.016	99.994	0.173	94.852
resnet9_8	91	0.017	99.992	0.174	94.862
resnet9_9	96	0.016	99.988	0.178	94.832

A SGD optimizer is used, and scheduled to linearly increase the learning rate on each step for the first 30 epochs to 1e-1. Then, a cosine annealing schedule follows for the remaining 70 epochs. The loss is determined using Categorical Cross Entropy. Results are reported in Tab. 2.

J. Training of ResNet-9 variants on CIFAR-10

The *ResNet-9* models were trained as detailed in Appendix I. However, the different random seed were provided for each model. Results are reported in Tab. 1.

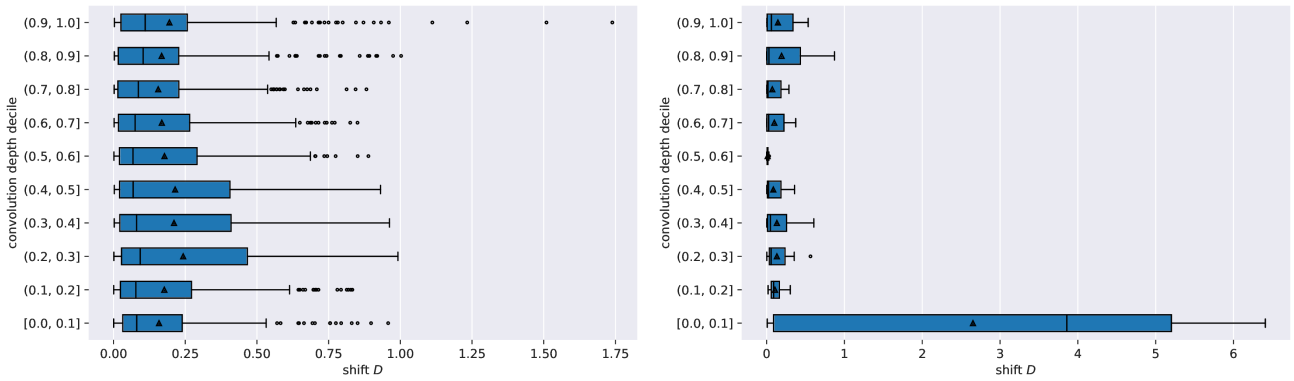

(a) GAN-Generator

(b) GAN-Discriminator

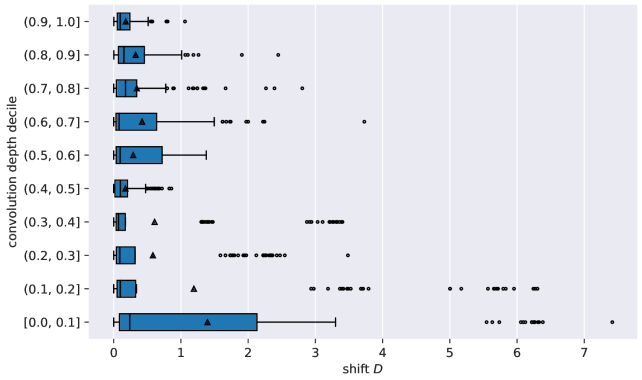

(c) Object Detection

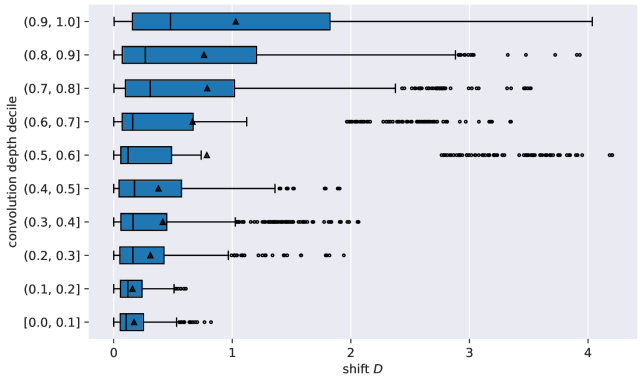

(d) Segmentation

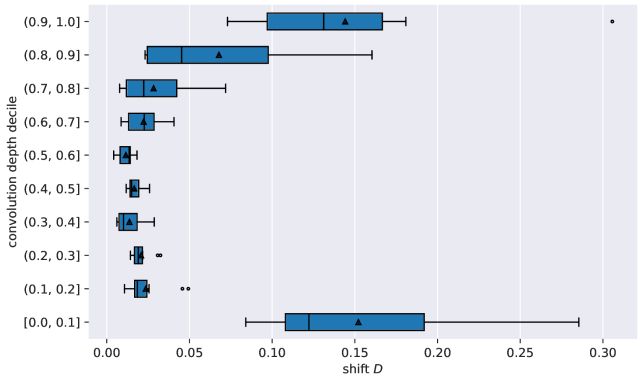

(e) Style Transfer

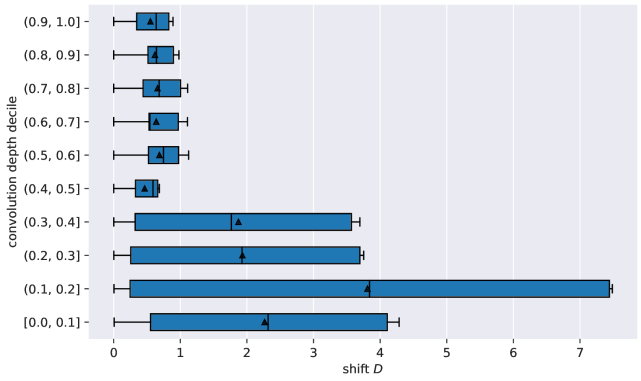

(f) Face Detection

Figure 9. Boxplots showing the distribution of pair-wise model-to-model shift D of models trained for various tasks per convolution depth decile. Note the change in scale of the x-axis.

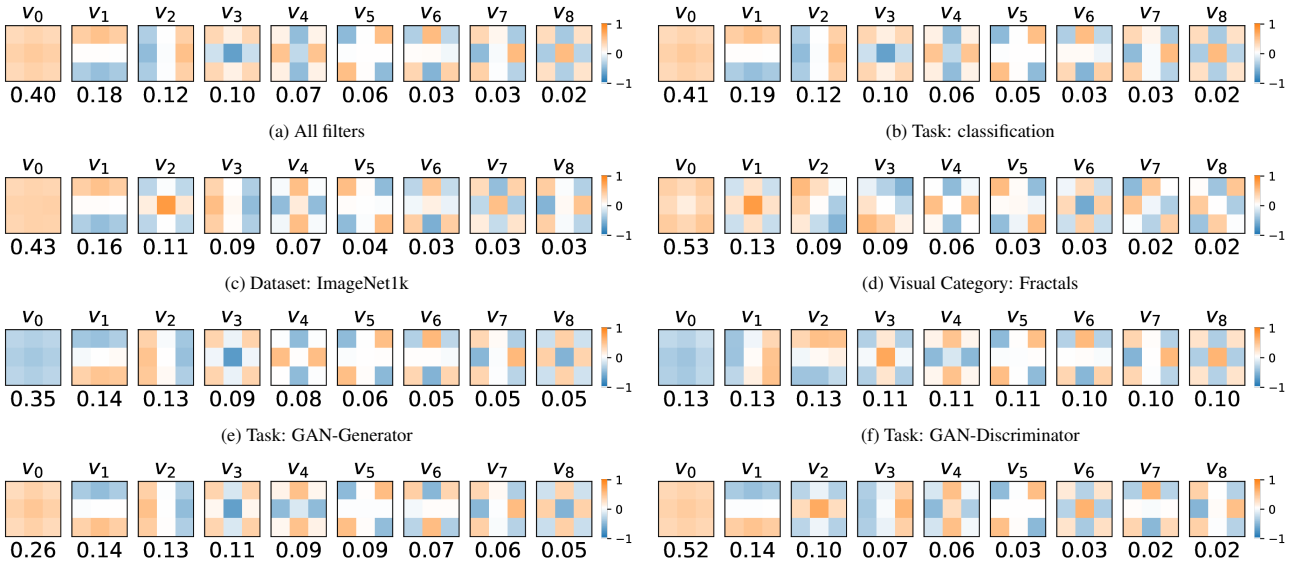

(a) All filters

(b) Task: classification

(c) Dataset: ImageNet1k

(d) Visual Category: Fractals

(e) Task: GAN-Generator

(f) Task: GAN-Discriminator

(g) First convolution layer

(h) Last convolution layers

Figure 10. Depiction of the filter basis and (cumulative) explained variance ratio per component for filters grouped by various meta-data dimensions.

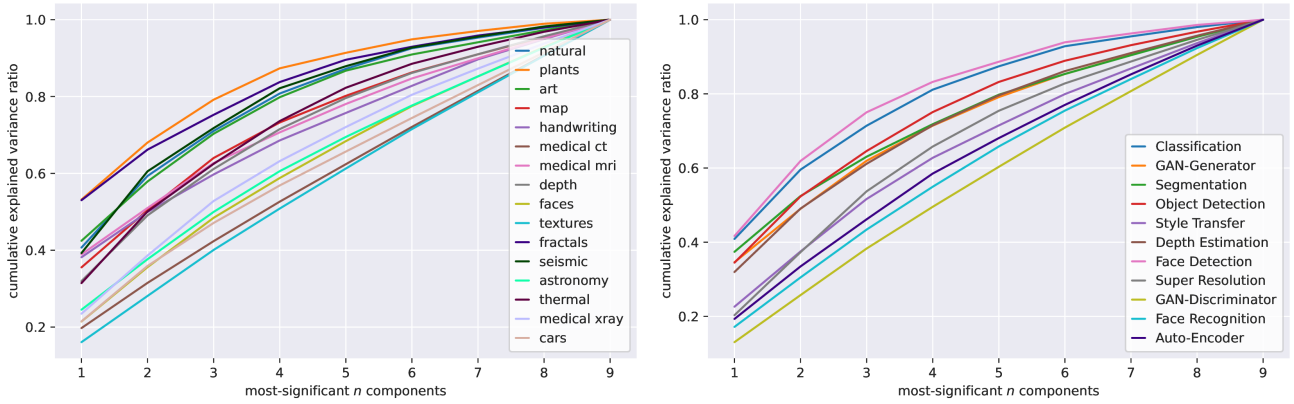

(a) visual category

(b) task

Figure 11. Cumulative ratio of explained variance over the first n components by all tasks and visual categories.

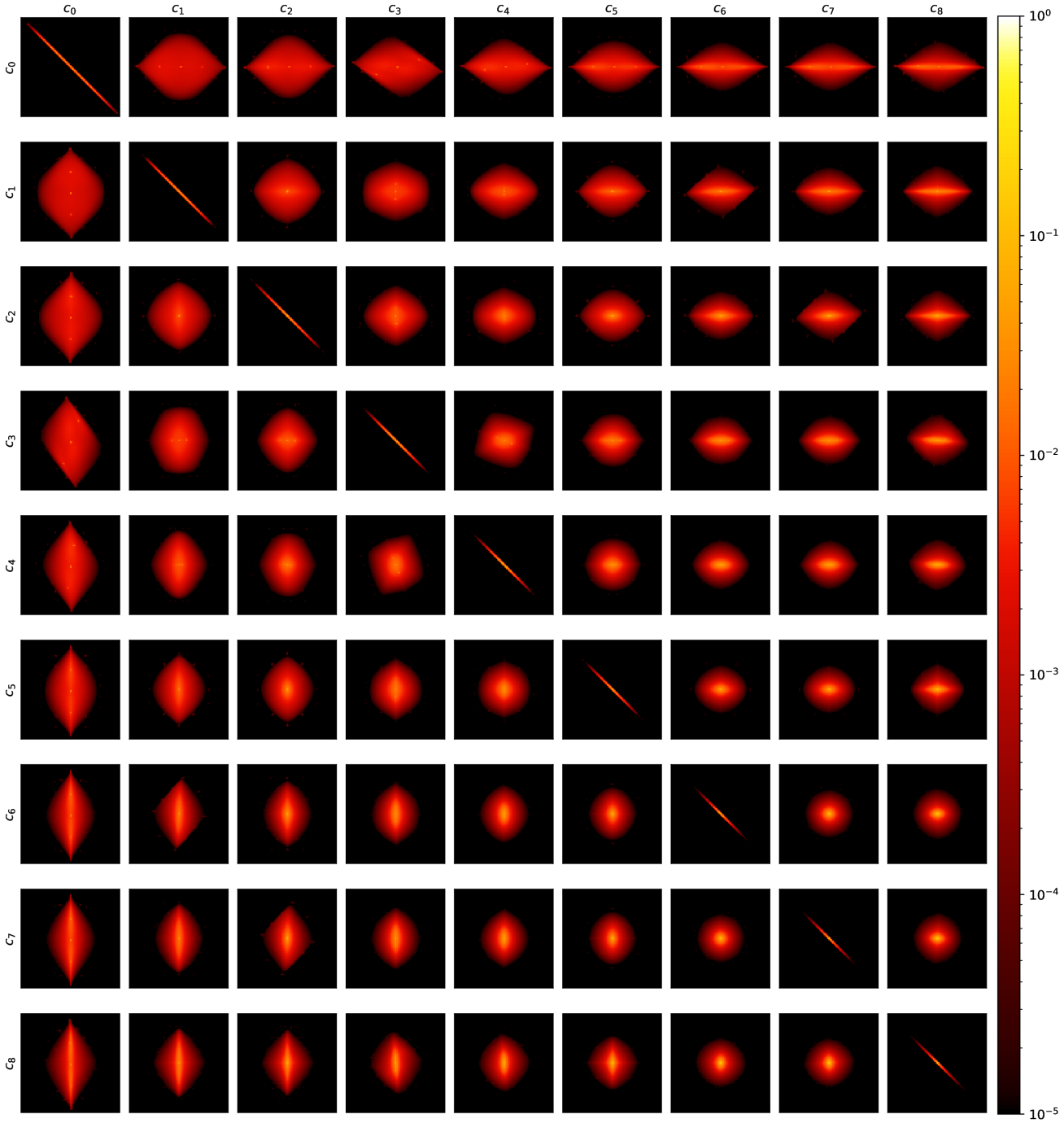

Figure 12. Bi-variate coefficient scatter plot over the full dataset.

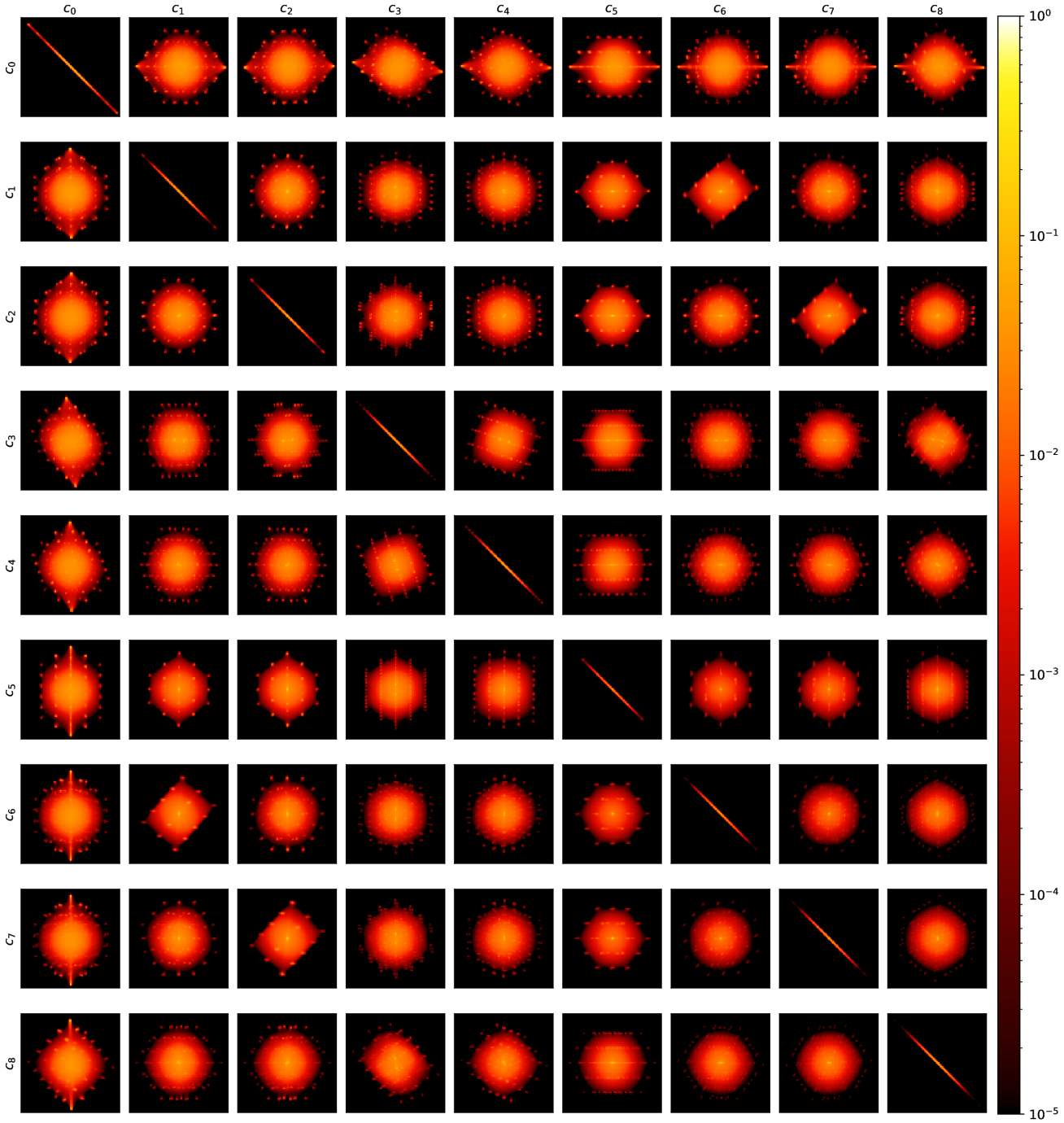

Figure 13. Bi-variate coefficient scatter plot of the phenotype *spikes*.

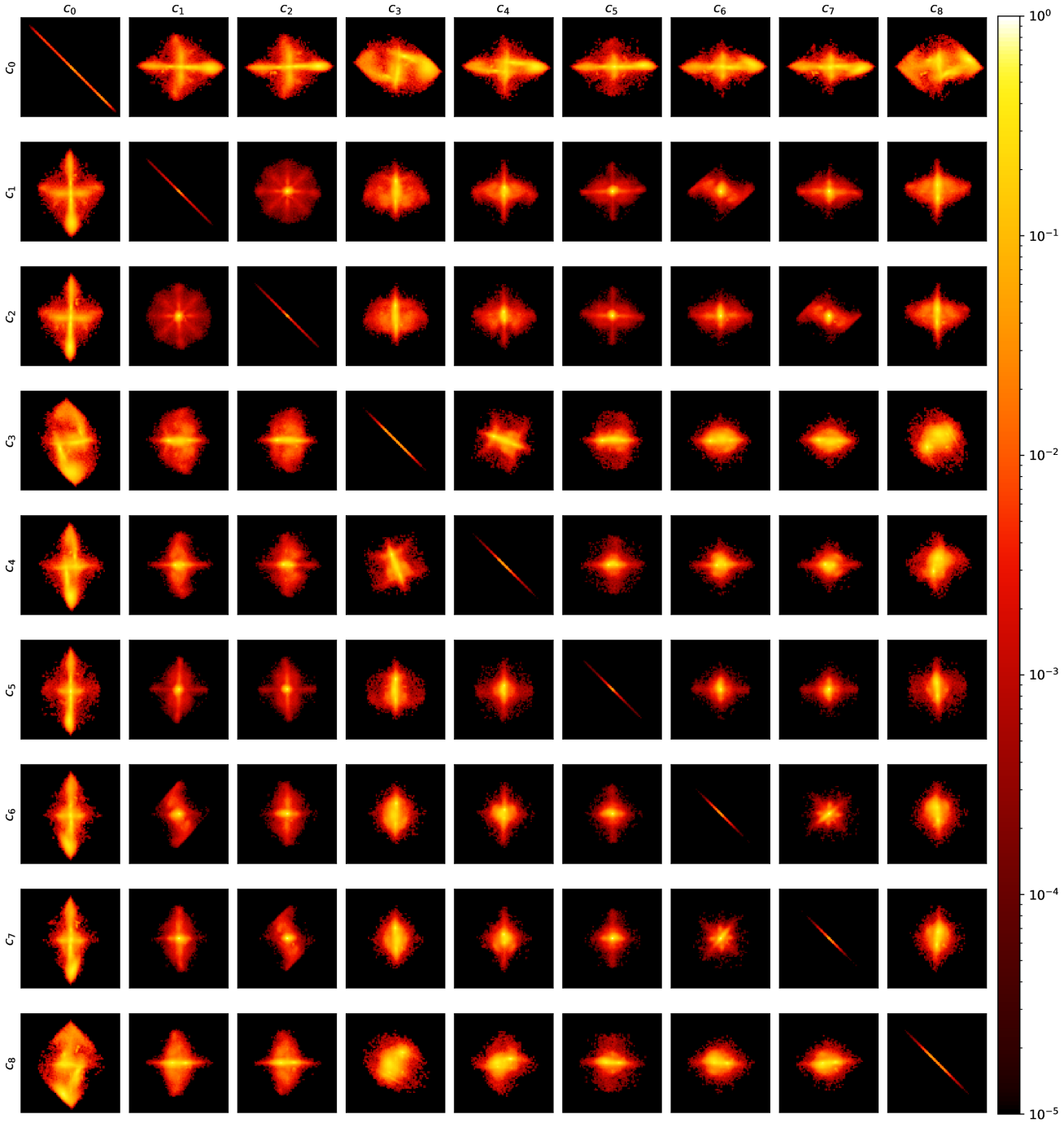

Figure 14. Bi-variate coefficient scatter plot of the phenotype *symbols*.

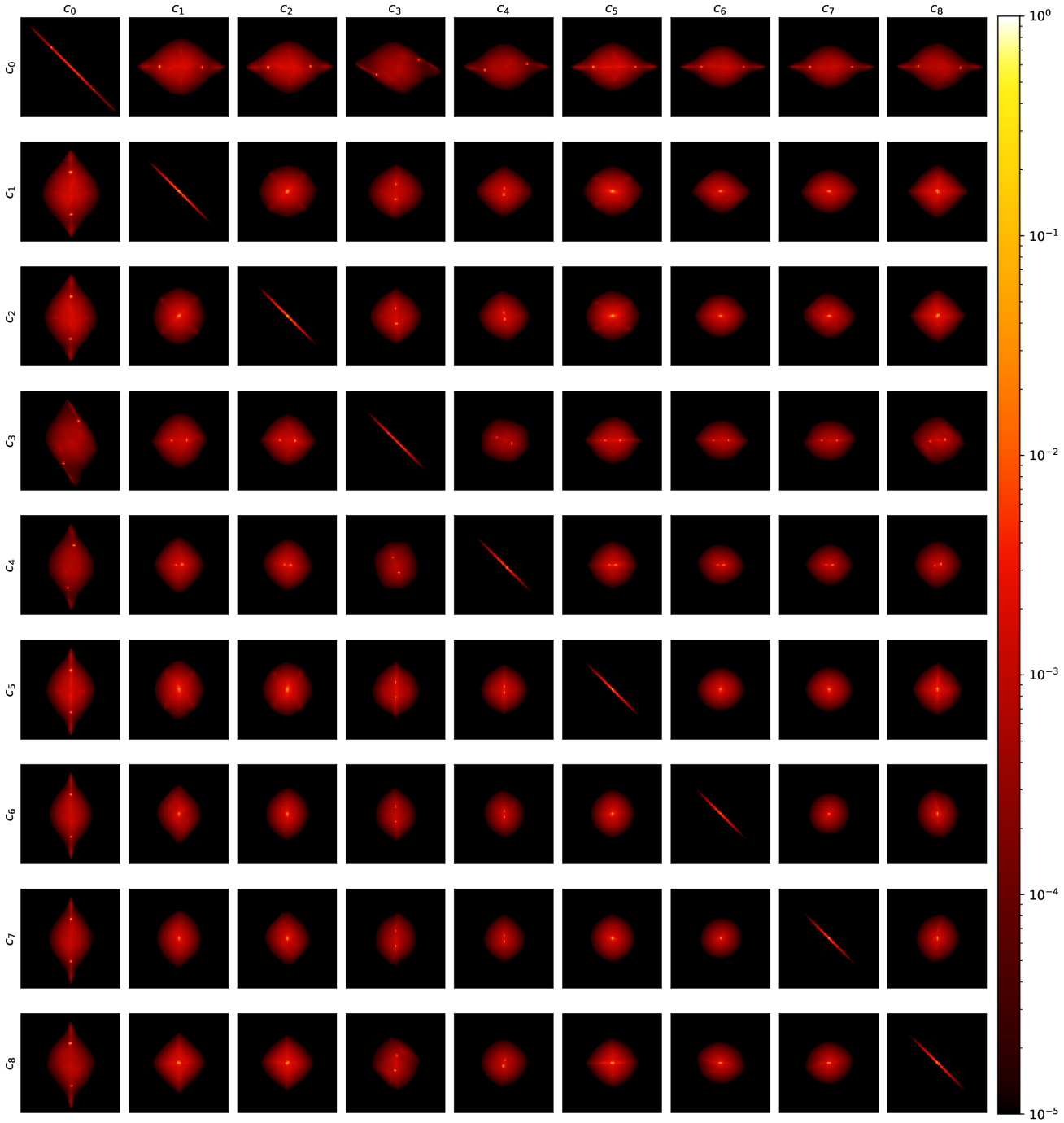

Figure 15. Bi-variate coefficient scatter plot of the phenotype *point*.

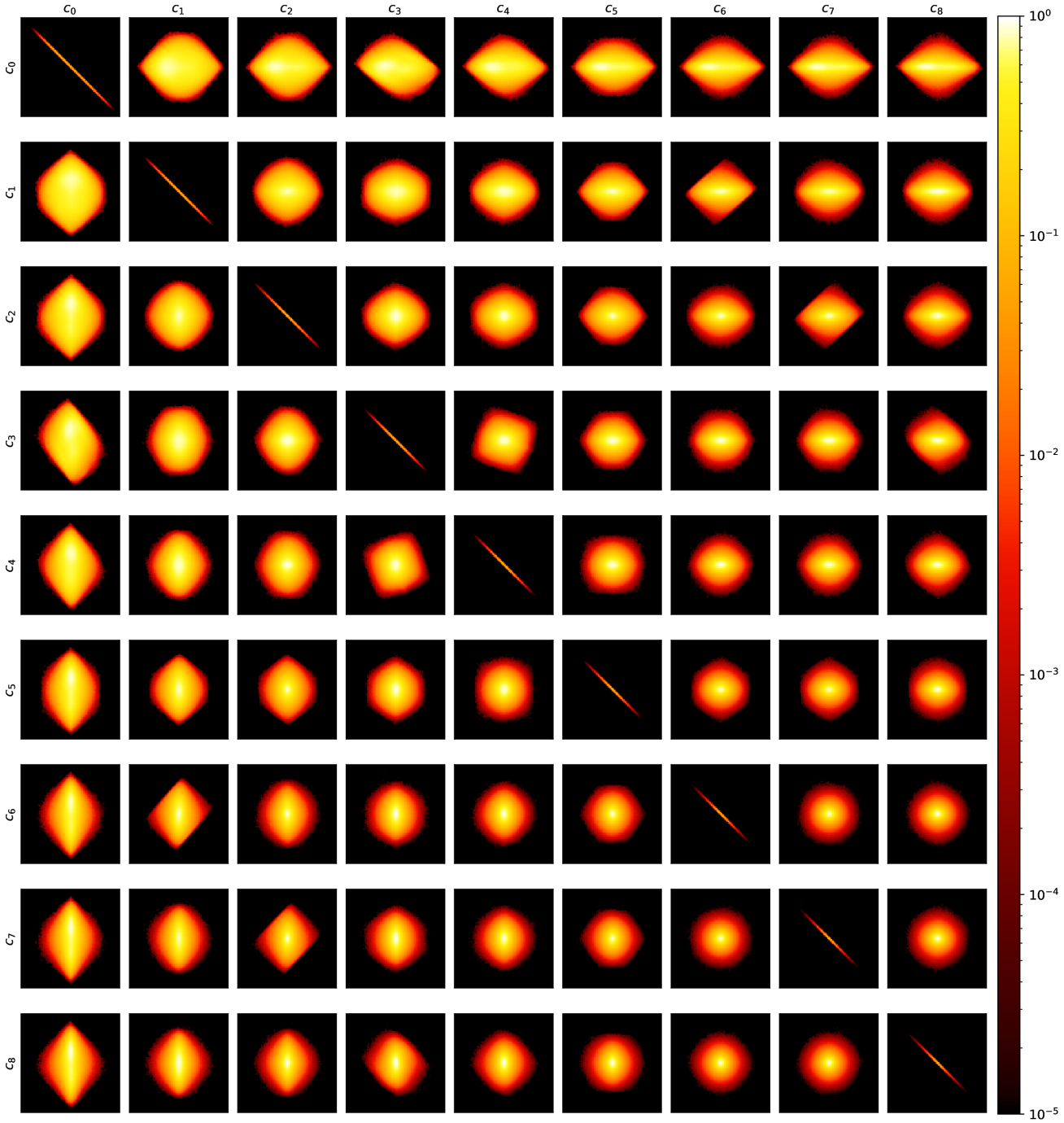

Figure 16. Bi-variate coefficient scatter plot of the phenotype *sun*.

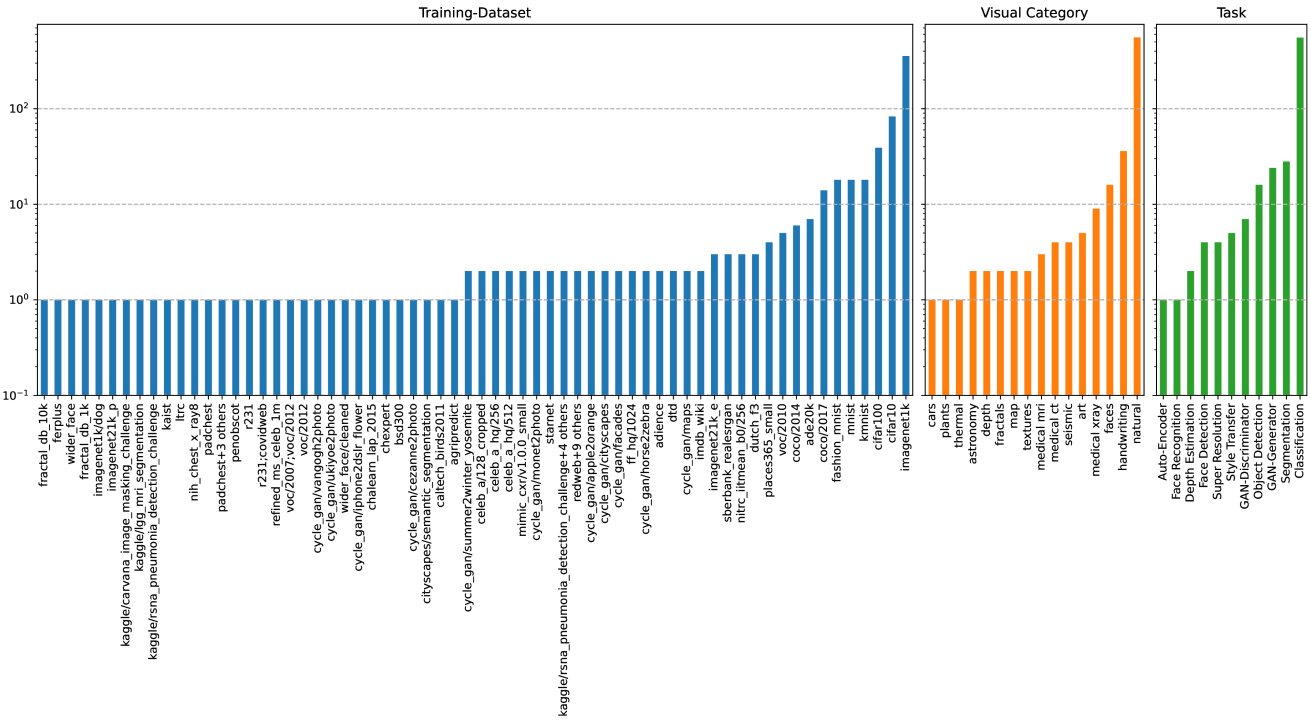

(a) model frequency

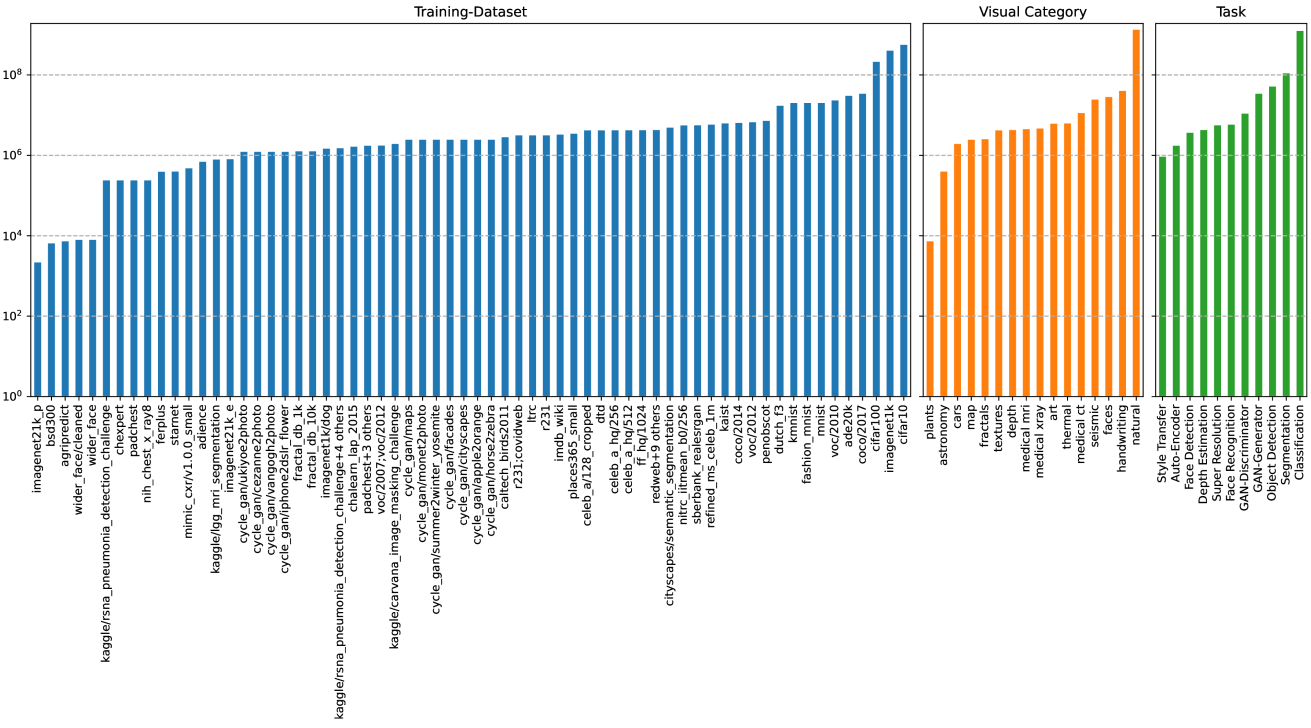

(b) filter frequency

Figure 17. Total frequency per filter sub-set. Log scale.

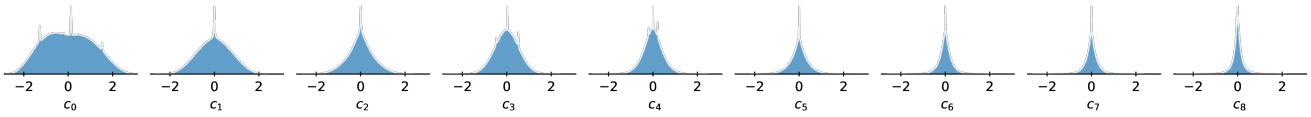

Figure 18. Distribution of the coefficients along the principal components of the **full dataset**.

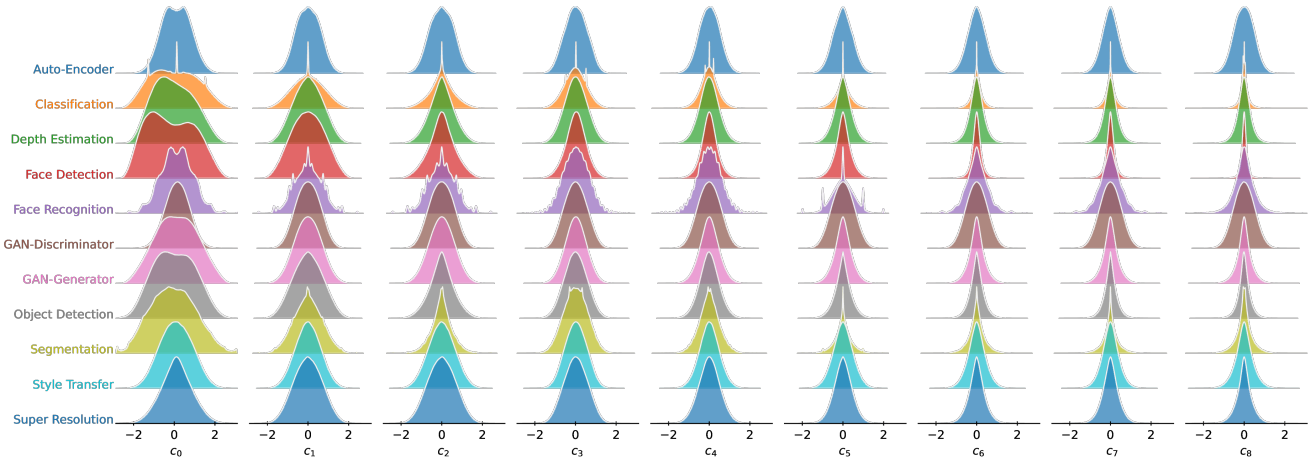

Figure 19. Distribution of the coefficients along the principal components by **model task**.

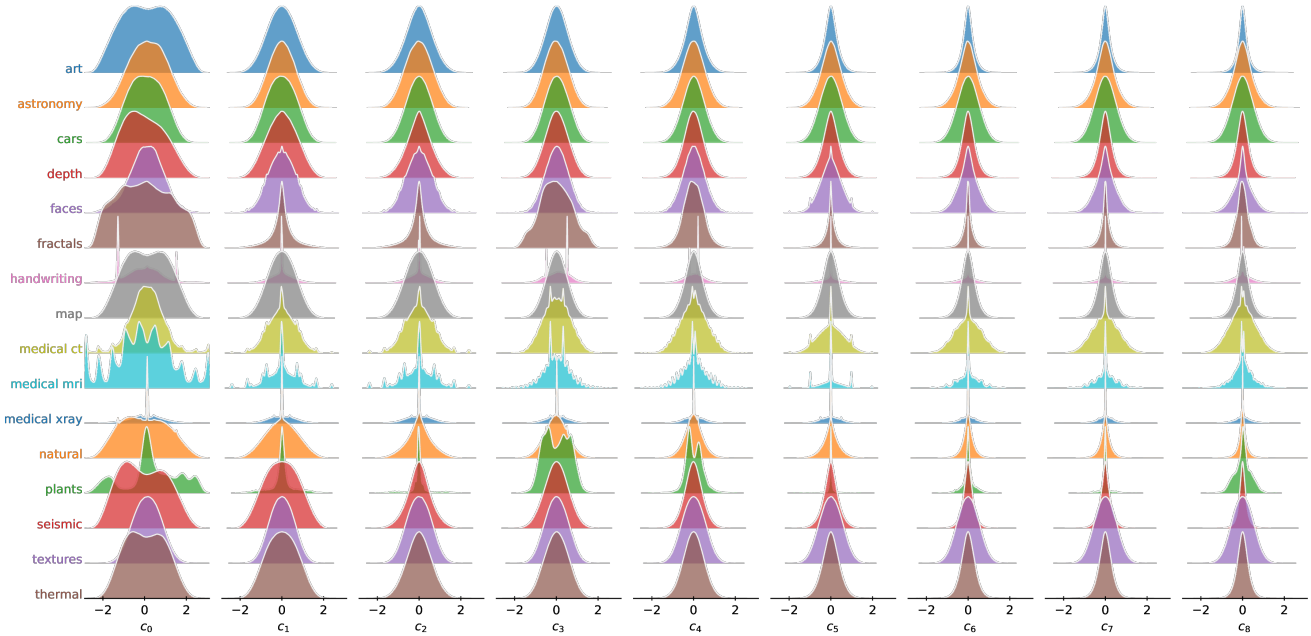

Figure 20. Distribution of the coefficients along the principal components by **visual category**.

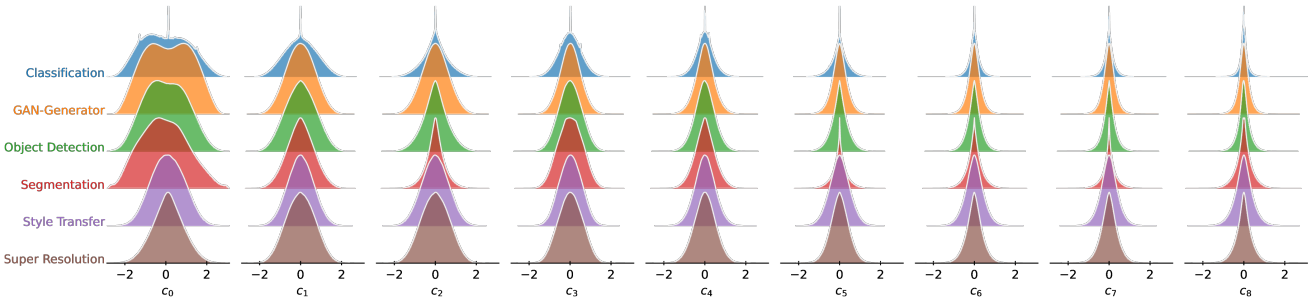

Figure 21. Distribution of the coefficients along the principal components by **model task for** datasets belonging to the **natural visual category.**

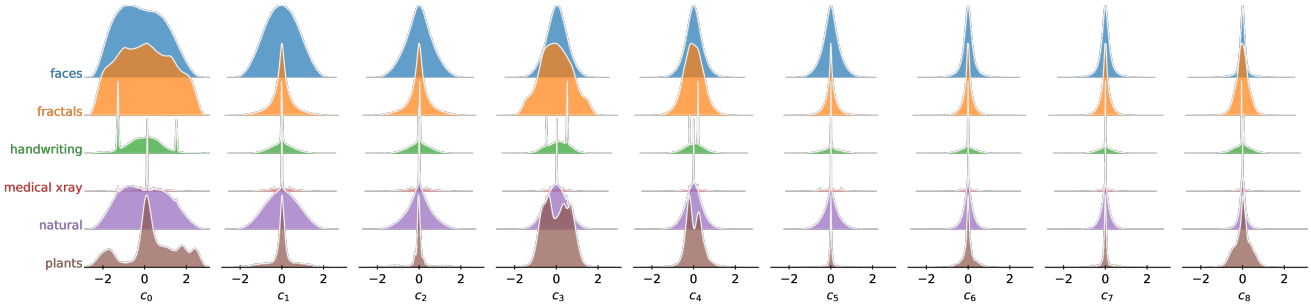

Figure 22. Distribution of the coefficients along the principal components by **visual training category for image classification models**.

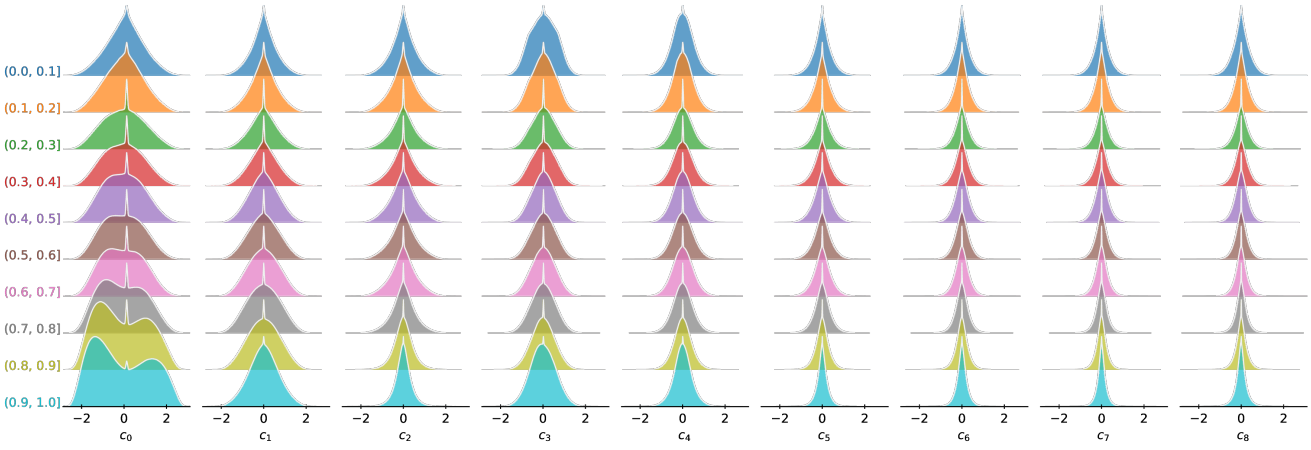

Figure 23. Distribution of the coefficients along the principal components by **convolution depth decile for image classification models**.

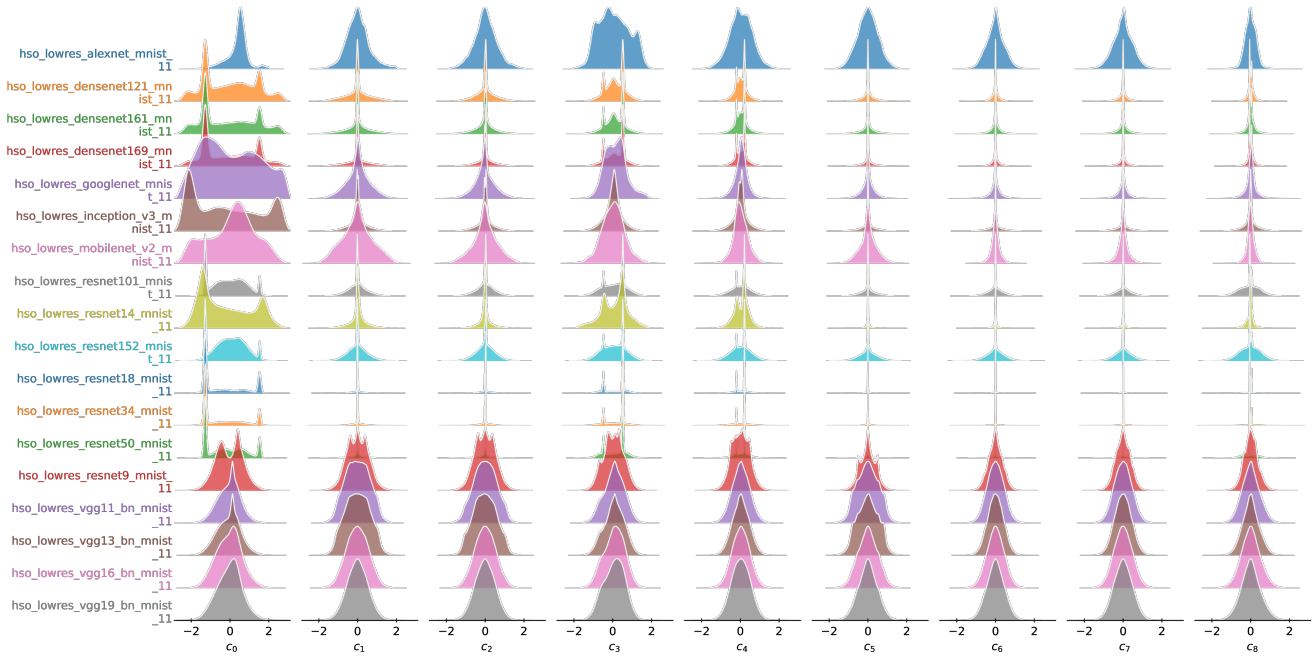

Figure 24. Distribution of the coefficients along the principal components of models trained on the **MNIST** dataset. All these models belong to our **intentionally overparameterized models**.

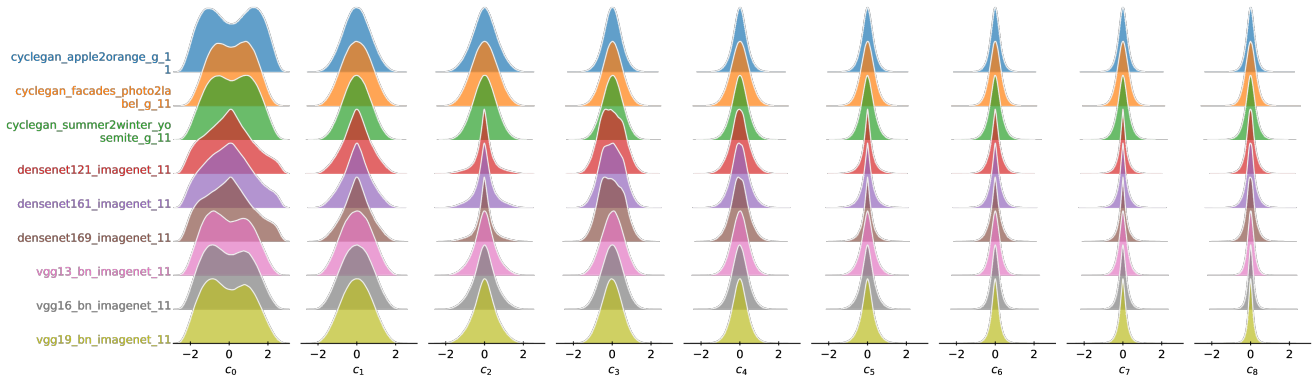

Figure 25. Distribution of the coefficients along the principal components of **selected models from similar families**.

Table 2. Performance of low resolution models with random seeds obtained after the validation epoch with the highest validation accuracy.

Dataset	Model	Best Epoch	Train Loss	Train Acc.	Val. Loss	Val. Acc.
cifar10	alexnet	95	0.563	80.717	0.604	79.297
cifar10	densenet121	96	0.047	99.716	0.247	93.780
cifar10	densenet161	97	0.042	99.830	0.232	94.311
cifar10	densenet169	98	0.046	99.742	0.235	94.171
cifar10	googlenet	97	0.064	99.651	0.242	92.919
cifar10	inception_v3	96	0.062	99.501	0.254	93.550
cifar10	mobilenet_v2	96	0.074	98.892	0.237	93.760
cifar10	resnet101	96	0.041	99.329	0.242	93.399
cifar10	resnet14	97	0.040	99.567	0.254	92.588
cifar10	resnet152	99	0.032	99.629	0.249	93.490
cifar10	resnet18	97	0.033	99.685	0.250	92.929
cifar10	resnet34	99	0.027	99.714	0.253	93.399
cifar10	resnet50	97	0.039	99.473	0.227	93.780
cifar10	resnet9	93	0.016	99.996	0.174	94.792
cifar10	vgg11_bn	95	0.024	99.860	0.254	92.258
cifar10	vgg13_bn	98	0.021	99.942	0.198	94.111
cifar10	vgg16_bn	99	0.021	99.912	0.228	93.930
cifar10	vgg19_bn	97	0.022	99.878	0.242	93.800
cifar100	densenet121	94	0.192	98.678	1.082	75.040
cifar100	densenet161	98	0.171	99.373	1.044	76.412
cifar100	densenet169	97	0.177	99.171	1.063	75.341
cifar100	googlenet	97	0.331	98.109	1.077	73.417
cifar100	inception_v3	97	0.276	98.395	1.055	75.040
cifar100	mobilenet_v2	93	0.342	94.940	1.009	75.200
cifar100	resnet101	95	0.133	98.596	1.070	74.740
cifar100	resnet14	98	0.380	93.321	1.110	70.673
cifar100	resnet152	97	0.127	98.846	1.059	74.720
cifar100	resnet18	98	0.163	98.257	1.103	72.536
cifar100	resnet34	97	0.103	99.165	1.161	72.546
cifar100	resnet50	96	0.131	98.834	1.062	74.159
cifar100	resnet9	91	0.075	99.806	1.000	75.591
cifar100	vgg11_bn	98	0.095	99.303	1.307	69.621
cifar100	vgg13_bn	94	0.088	99.393	1.158	73.017
cifar100	vgg16_bn	96	0.110	98.702	1.267	72.907
cifar100	vgg19_bn	96	0.136	97.917	1.349	71.945
mnist	alexnet	86	0.053	98.444	0.045	98.668
mnist	densenet121	92	0.035	99.980	0.044	99.579
mnist	densenet161	93	0.035	99.983	0.043	99.609
mnist	densenet169	96	0.036	99.977	0.042	99.649
mnist	googlenet	90	0.046	99.873	0.045	99.579
mnist	inception_v3	98	0.046	99.873	0.041	99.679
mnist	mobilenet_v2	96	0.035	99.983	0.042	99.659
mnist	resnet101	87	0.020	99.978	0.032	99.539
mnist	resnet14	80	0.021	99.985	0.030	99.669
mnist	resnet152	94	0.019	99.990	0.030	99.589
mnist	resnet18	83	0.020	99.993	0.030	99.639
mnist	resnet34	79	0.019	99.977	0.029	99.609
mnist	resnet50	86	0.020	99.982	0.032	99.559
mnist	resnet9	83	0.006	99.998	0.016	99.679
mnist	vgg11_bn	75	0.017	99.995	0.027	99.639
mnist	vgg13_bn	90	0.017	99.998	0.026	99.649
mnist	vgg16_bn	90	0.017	99.992	0.026	99.639
mnist	vgg19_bn	85	0.017	99.988	0.027	99.649
kmnist	alexnet	97	0.047	98.775	0.191	94.872
kmnist	densenet121	88	0.037	99.982	0.092	98.668
kmnist	densenet161	87	0.038	99.972	0.084	98.688
kmnist	densenet169	89	0.037	99.987	0.096	98.518
kmnist	googlenet	97	0.044	99.970	0.112	97.947
kmnist	inception_v3	97	0.044	99.970	0.090	98.658

Continued on next page

Dataset	Model	Best Epoch	Train Loss	Train Acc.	Val. Loss	Val. Acc.
kmnist	mobilenet_v2	89	0.036	99.988	0.095	98.468
kmnist	resnet101	90	0.020	99.993	0.097	98.147
kmnist	resnet14	73	0.021	99.975	0.070	98.748
kmnist	resnet152	85	0.020	99.988	0.090	98.197
kmnist	resnet18	73	0.020	99.997	0.077	98.628
kmnist	resnet34	83	0.018	99.998	0.081	98.538
kmnist	resnet50	80	0.020	99.982	0.097	98.067
kmnist	resnet9	54	0.008	99.997	0.069	98.528
kmnist	vgg11_bn	62	0.016	99.998	0.078	98.427
kmnist	vgg13_bn	54	0.016	99.980	0.069	98.698
kmnist	vgg16_bn	79	0.015	99.998	0.070	98.698
kmnist	vgg19_bn	99	0.015	99.998	0.078	98.518
fashionmnist	alexnet	97	0.296	89.248	0.308	89.042
fashionmnist	densenet121	92	0.037	99.947	0.266	93.950
fashionmnist	densenet161	93	0.038	99.937	0.264	94.171
fashionmnist	densenet169	97	0.038	99.933	0.258	94.291
fashionmnist	googlenet	96	0.044	99.973	0.240	93.439
fashionmnist	inception_v3	97	0.050	99.861	0.244	94.441
fashionmnist	mobilenet_v2	98	0.040	99.913	0.252	93.860
fashionmnist	resnet101	94	0.019	99.985	0.281	93.740
fashionmnist	resnet14	89	0.021	99.997	0.228	94.040
fashionmnist	resnet152	91	0.020	99.970	0.286	93.770
fashionmnist	resnet18	86	0.020	99.998	0.228	93.970
fashionmnist	resnet34	96	0.018	99.993	0.261	93.910
fashionmnist	resnet50	89	0.019	99.985	0.261	93.810
fashionmnist	resnet9	63	0.009	99.998	0.203	94.071
fashionmnist	vgg11_bn	91	0.017	100.000	0.229	93.600
fashionmnist	vgg13_bn	80	0.017	99.998	0.211	94.111
fashionmnist	vgg16_bn	86	0.018	99.995	0.226	94.030
fashionmnist	vgg19_bn	95	0.018	99.987	0.244	93.960

Table 3. Description of columns present in the meta data.

Column	Values	Description
model_id	int	Unique ID of the model.
conv_depth	int	Convolution depth of the extracted filter i.e. how many convolution layers were hierarchically below the layer, that this filter was extracted from.
conv_depth_norm	float	Similar to conv_depth but normalized by the maximum conv_depth. Will be a float between 0 (first layers) . . . , 1 (towards head).
filter_ids	list of ints	List of Filter IDs that belong to this record. These can directly be mapped to the rows of the filter array.
model	str	Unique string ID of the model. Typically, but not reliably in the format `{name}_{trainingset}_{onnx opset}`.
producer	str	Producer of the ONNX export. Typically various versions of PyTorch.
op_set	int	Version of the ONNX operator set used for export.
depth	int	Total hierarchical depth of the model including all layers.
Name	str	Name of the model.
Paper	str	Link to the original publication.
Pretraining-Dataset	str	Name of the pretraining dataset(s) if pretrained. Combined datasets are separated by commas.
Training-Dataset	str	Name of the training dataset(s). Combined datasets are separated by commas.
Visual Category	str	Visual, manual categorization of the training datasets.
Task	str	Task of the model.
Accessible	str	Represents where the model can be found. Typically, this will be a link to GitHub.
Dataset URL	str	URL of the training dataset. Usually only entered for exotic datasets.
total_filters	int	Total number of convolution filters in this model.
`(X, Y)` filters	int	Represents frequency of filters with shape `(X, Y)` were found in the processed model.
`onnx_operator` (e.g. Conv, Add, Relu, MaxPool)	int	Represents frequency of this particular ONNX operator was found in the processed model. Please note that individual operators may have been fused in later ONNX operator sets.

Table 4. List of all collected models. Mainly sourced from [2–4]. Where possible, the dataset IDs correspond to the *TensorFlow* naming [5]. Models that start with *hso_* denote out intentionally overparametrized models (**h**ighly **s**parse and **o**verparametrized).

Model ID	**Pretraining-Dataset**	**Training-Dataset(s)**	**Task**	**Visual Category**	3×3 **Filters**
agripredict_disease_classification_prop_11 [6]	-	agripredict	Classification	plants	7232
cyclegan_horse2zebra_g_11 [7]	-	cycle_gan/horse2zebra	GAN-Generator	natural	1220608
cyclegan_monet2photo_g_11 [7]	-	cycle_gan/monet2photo	GAN-Generator	art	1220608
cyclegan_facades_label2photo_g_11 [7]	-	cycle_gan/facades	GAN-Generator	natural	1220608
cyclegan_style_cezanne_g_11 [7]	-	cycle_gan/cezanne2photo	GAN-Generator	art	1220608
cyclegan_summer2winter_yosemite_g_11 [7]	-	cycle_gan/summer2winter_yosemite	GAN-Generator	natural	1220608
cyclegan_apple2orange_g_11 [7]	-	cycle_gan/apple2orange	GAN-Generator	natural	1220608
cyclegan_cityscapes_photo2label_g_11 [7]	-	cycle_gan/cityscapes	GAN-Generator	natural	1220608
cyclegan_zebra2horse_g_11 [7]	-	cycle_gan/horse2zebra	GAN-Generator	natural	1220608
cyclegan_map2sat_g_11 [7]	-	cycle_gan/maps	GAN-Generator	map	1220608
cyclegan_iphone2dslr_flower_g_11 [7]	-	cycle_gan/iphone2dslr_flower	GAN-Generator	natural	1220608
cyclegan_facades_photo2label_g_11 [7]	-	cycle_gan/facades	GAN-Generator	natural	1220608
cyclegan_cityscapes_label2photo_g_11 [7]	-	cycle_gan/cityscapes	GAN-Generator	natural	1220608
cyclegan_orange2apple_g_11 [7]	-	cycle_gan/apple2orange	GAN-Generator	natural	1220608
cyclegan_style_ukiyoe_g_11 [7]	-	cycle_gan/ukiyoe2photo	GAN-Generator	art	1220608
cyclegan_style_vangogh_g_11 [7]	-	cycle_gan/vangogh2photo	GAN-Generator	art	1220608
cyclegan_winter2summer_yosemite_g_11 [7]	-	cycle_gan/summer2winter_yosemite	GAN-Generator	natural	1220608
cyclegan_sat2map_g_11 [7]	-	cycle_gan/maps	GAN-Generator	map	1220608
cyclegan_style_monet_g_11 [7]	-	cycle_gan/monet2photo	GAN-Generator	art	1220608
densenet161_places365_11 [8]	-	places365_small	Classification	natural	718848
ghostnet_1x_imagenet_11 [9]	-	imagenet1k	Classification	natural	4616
hardnet39ds_imagenet_11 [10]	-	imagenet1k	Classification	natural	3752
alexnet_places365_11 [8]	-	places365_small	Classification	natural	237568
hardnet68ds_imagenet_11 [10]	-	imagenet1k	Classification	natural	5090
hardnet68_imagenet_11 [10]	-	imagenet1k	Classification	natural	1680056
hso_lowres_alexnet_cifar10_11 [11]	-	cifar10	Classification	natural	250048
hso_lowres_densenet121_cifar100_11 [12]	-	cifar100	Classification	natural	237760
hardnet85_imagenet_11 [10]	-	imagenet1k	Classification	natural	3625760
hso_lowres_alexnet_fashionmnist_11 [11]	-	fashion_mnist	Classification	natural	249920
hso_lowres_alexnet_kmnist_11 [11]	-	kmnist	Classification	handwriting	249920
hso_lowres_densenet121_cifar10_11 [12]	-	cifar10	Classification	natural	237760
hso_lowres_densenet121_fashionmnist_11 [12]	-	fashion_mnist	Classification	natural	237632
hso_lowres_alexnet_mnist_11 [11]	-	mnist	Classification	handwriting	249920
hso_lowres_densenet121_kmnist_11 [12]	-	kmnist	Classification	handwriting	237632
hso_lowres_densenet121_mnist_11 [12]	-	mnist	Classification	handwriting	237632
compnet_weights_sagittal_improvement_09_NITRC_IITmean_b0_256_12 [13]	-	nitrc_iitmean_b0/256	Segmentation	medical ct	1842688
compnet_weights_coronal_improvement_08_NITRC_IITmean_b0_256_12 [13]	-	nitrc_iitmean_b0/256	Segmentation	medical mri	1842688

Continued on next page

Model ID	Pretraining-Dataset	Training-Dataset	Task	Visual Category	3×3 Filters
compnet_weights_axial_improvement_08_NITRC_IITmean_b0_256_12 [13]	-	nitrc_iitmean_b0/256	Segmentation	medical mri	1842688
hso_lowres_densenet161_cifar100_11 [12]	-	cifar100	Classification	natural	719136
hso_lowres_googlenet_cifar100_11 [14]	-	cifar100	Classification	natural	356672
hso_lowres_densenet169_fashionmnist_11 [12]	-	fashion_mnist	Classification	natural	335936
hso_lowres_densenet169_cifar100_11 [12]	-	cifar100	Classification	natural	336064
hso_lowres_googlenet_fashionmnist_11 [14]	-	fashion_mnist	Classification	natural	356288
hso_lowres_googlenet_cifar10_11 [14]	-	cifar10	Classification	natural	356672
hso_lowres_densenet169_kmnist_11 [12]	-	kmnist	Classification	handwriting	335936
hso_lowres_densenet161_cifar10_11 [12]	-	cifar10	Classification	natural	719136
hso_lowres_densenet169_cifar10_11 [12]	-	cifar10	Classification	natural	336064
hso_lowres_densenet161_fashionmnist_11 [12]	-	fashion_mnist	Classification	natural	718944
hso_lowres_densenet169_mnist_11 [12]	-	mnist	Classification	handwriting	335936
hso_lowres_densenet161_kmnist_11 [12]	-	kmnist	Classification	handwriting	718944
hso_lowres_densenet161_mnist_11 [12]	-	mnist	Classification	handwriting	718944
hso_lowres_googlenet_kmnist_11 [14]	-	kmnist	Classification	handwriting	356288
hso_lowres_googlenet_mnist_11 [14]	-	mnist	Classification	handwriting	356288
facebook_detr_resnet_50_coco2017_12 [15]	-	coco/2017	Object Detection	natural	1257472
hso_lowres_mobilenet_v2_fashionmnist_11 [16]	-	fashion_mnist	Classification	natural	7168
hso_lowres_mobilenet_v2_kmnist_11 [16]	-	kmnist	Classification	handwriting	7168
hso_lowres_mobilenet_v2_cifar10_11 [16]	-	cifar10	Classification	natural	7232
hso_lowres_mobilenet_v2_cifar100_11 [16]	-	cifar100	Classification	natural	7232
hso_lowres_mobilenet_v2_mnist_11 [16]	-	mnist	Classification	handwriting	7168
hso_lowres_inception_v3_cifar100_11 [17]	-	cifar100	Classification	natural	614976
hso_lowres_inception_v3_cifar10_11 [17]	-	cifar10	Classification	natural	614976
hso_lowres_inception_v3_fashionmnist_11 [17]	-	fashion_mnist	Classification	natural	614592
hso_lowres_inception_v3_kmnist_11 [17]	-	kmnist	Classification	handwriting	614592
hso_lowres_inception_v3_mnist_11 [17]	-	mnist	Classification	handwriting	614592
facebook_detr_resnet_50_dc5_panoptic_coco2017_12 [15]	-	coco/2017	Segmentation	natural	1371728
facebook_detr_resnet_50_panoptic_coco2017_12 [15]	-	coco/2017	Segmentation	natural	1371728
facebook_detr_resnet_50_dc5_coco2017_12 [15]	-	coco/2017	Object Detection	natural	1257472
hso_lowres_resnet101_cifar100_11 [18]	-	cifar100	Classification	natural	2371776
hso_lowres_resnet14_cifar100_11 [18]	-	cifar100	Classification	natural	303296
hso_lowres_resnet101_cifar10_11 [18]	-	cifar10	Classification	natural	2371776
hso_lowres_resnet14_cifar10_11 [18]	-	cifar10	Classification	natural	303296
hso_lowres_resnet14_fashionmnist_11 [18]	-	fashion_mnist	Classification	natural	303168
hso_lowres_resnet14_kmnist_11 [18]	-	kmnist	Classification	handwriting	303168
hso_lowres_resnet101_fashionmnist_11 [18]	-	fashion_mnist	Classification	natural	2371648
hso_lowres_resnet14_mnist_11 [18]	-	mnist	Classification	handwriting	303168
hso_lowres_resnet101_kmnist_11 [18]	-	kmnist	Classification	handwriting	2371648
hso_lowres_resnet101_mnist_11 [18]	-	mnist	Classification	handwriting	2371648
hso_lowres_resnet152_cifar100_11 [18]	-	cifar100	Classification	natural	3289280
hso_lowres_resnet18_cifar100_11 [18]	-	cifar100	Classification	natural	1220800
hso_lowres_resnet152_cifar10_11 [18]	-	cifar10	Classification	natural	3289280
hso_lowres_resnet18_cifar10_11 [18]	-	cifar10	Classification	natural	1220800
hso_lowres_resnet18_fashionmnist_11 [18]	-	fashion_mnist	Classification	natural	1220672
hso_lowres_resnet18_kmnist_11 [18]	-	kmnist	Classification	handwriting	1220672
hso_lowres_resnet152_fashionmnist_11 [18]	-	fashion_mnist	Classification	natural	3289152
hso_lowres_resnet152_mnist_11 [18]	-	mnist	Classification	handwriting	3289152
hso_lowres_resnet152_kmnist_11 [18]	-	kmnist	Classification	handwriting	3289152
hso_lowres_resnet18_mnist_11 [18]	-	mnist	Classification	handwriting	1220672
hso_lowres_resnet34_cifar100_11 [18]	-	cifar100	Classification	natural	2343104
hso_lowres_resnet34_cifar10_11 [18]	-	cifar10	Classification	natural	2343104
hso_lowres_resnet34_mnist_11 [18]	-	mnist	Classification	handwriting	2342976
hso_lowres_resnet34_fashionmnist_11 [18]	-	fashion_mnist	Classification	natural	2342976
hso_lowres_resnet34_kmnist_11 [18]	-	kmnist	Classification	handwriting	2342976
hso_lowres_resnet50_cifar100_11 [18]	-	cifar100	Classification	natural	1257664
hso_lowres_resnet50_cifar10_11 [18]	-	cifar10	Classification	natural	1257664
hso_lowres_resnet50_fashionmnist_11 [18]	-	fashion_mnist	Classification	natural	1257536
hso_lowres_resnet50_kmnist_11 [18]	-	kmnist	Classification	handwriting	1257536
hso_lowres_resnet50_mnist_11 [18]	-	mnist	Classification	handwriting	1257536

Continued on next page

Model ID	Pretraining-Dataset	Training-Dataset	Task	Visual Category	3×3 Filters
hso_lowres_resnet9_cifar100_11 [18]	-	cifar100	Classification	natural	729280
hso_lowres_resnet9_cifar10_11 [18]	-	cifar10	Classification	natural	729280
hso_lowres_resnet9_fashionmnist_11 [18]	-	fashion_mnist	Classification	natural	729152
hso_lowres_resnet9_kmnist_11 [18]	-	kmnist	Classification	handwriting	729152
hso_lowres_resnet9_mnist_11 [18]	-	mnist	Classification	handwriting	729152
hso_lowres_vgg11_bn_cifar10_11 [19]	-	cifar10	Classification	natural	1024192
hso_lowres_vgg11_bn_cifar100_11 [19]	-	cifar100	Classification	natural	1024192
hso_lowres_vgg11_bn_fashionmnist_11 [19]	-	fashion_mnist	Classification	natural	1024064
hso_lowres_vgg11_bn_kmnist_11 [19]	-	kmnist	Classification	handwriting	1024064
hso_lowres_vgg11_bn_mnist_11 [19]	-	mnist	Classification	handwriting	1024064
hso_lowres_vgg13_bn_cifar100_11 [19]	-	cifar100	Classification	natural	1044672
hso_lowres_vgg13_bn_cifar10_11 [19]	-	cifar10	Classification	natural	1044672
hso_lowres_vgg13_bn_fashionmnist_11 [19]	-	fashion_mnist	Classification	natural	1044544
hso_lowres_vgg13_bn_kmnist_11 [19]	-	kmnist	Classification	handwriting	1044544
hso_lowres_vgg13_bn_mnist_11 [19]	-	mnist	Classification	handwriting	1044544
hso_lowres_vgg16_bn_fashionmnist_11 [19]	-	fashion_mnist	Classification	natural	1634368
hso_lowres_vgg16_bn_cifar100_11 [19]	-	cifar100	Classification	natural	1634496
hso_lowres_vgg16_bn_cifar10_11 [19]	-	cifar10	Classification	natural	1634496
hso_lowres_vgg16_bn_kmnist_11 [19]	-	kmnist	Classification	handwriting	1634368
hso_lowres_vgg16_bn_mnist_11 [19]	-	mnist	Classification	handwriting	1634368
hso_lowres_vgg19_bn_cifar100_11 [19]	-	cifar100	Classification	natural	2224320
hso_lowres_vgg19_bn_cifar10_11 [19]	-	cifar10	Classification	natural	2224320
hso_lowres_vgg19_bn_fashionmnist_11 [19]	-	fashion_mnist	Classification	natural	2224192
hso_lowres_vgg19_bn_kmnist_11 [19]	-	kmnist	Classification	handwriting	2224192
hso_lowres_vgg19_bn_mnist_11 [19]	-	mnist	Classification	handwriting	2224192
lungmask_unet_LTRCLobes_11 [20]	-	ltrc	Segmentation	medical ct	3137600
lungmask_unet_R231CovidWeb_11 [20]	-	r231, covidweb	Segmentation	medical ct	3137600
lungmask_unet_R231_11 [20]	-	r231	Segmentation	medical ct	3137600
mealv1_resnest50_imagenet_11 [21]	-	imagenet1k	Classification	natural	1257472
mealv2_efficientnet_b0_imagenet_11 [21]	-	imagenet1k	Classification	natural	2720
mealv2_mobilenet_v3_large_100_imagenet_11 [21]	-	imagenet1k	Classification	natural	2160
mealv2_mobilenetv3_small_075_imagenet_11 [21]	-	imagenet1k	Classification	natural	224
mealv2_mobilenetv3_small_100_imagenet_11 [21]	-	imagenet1k	Classification	natural	224
mealv2_resnest50_380x380_imagenet_11 [21]	-	imagenet1k	Classification	natural	1257472
mealv2_resnest50_cutmix_imagenet_11 [21]	-	imagenet1k	Classification	natural	1257472
mealv2_resnest50_imagenet_11 [21]	-	imagenet1k	Classification	natural	1257472
candy-9 [22]	-	coco/2014	Style Transfer	natural	184320
midas_small_redweb_diml_movies_megadepth_wsvd_tartanair_hrwsi_apolloscape_blendedmvs_irs_11 [23]	-	redweb, diml, movies, megadepth, wsvd, tartanair, hrwsi, apolloscape, blendedmvs, irs	Depth Estimation	depth	1115680
efficientnet-lite4-11 [24]	-	coco/2017	Classification	natural	6176
ntsnet_cub2002011_11 [25]	-	caltech_birds2011	Classification	natural	2809856
mosaic-9 [22]	-	coco/2014	Style Transfer	natural	184320
age_googlenet [26]	-	adience	Classification	natural	344576
pointilism-9 [22]	-	coco/2014	Style Transfer	natural	184320
emotion-ferplus-8 [27]	-	ferplus	Classification	faces	389184
rain-princess-9 [22]	-	coco/2014	Style Transfer	natural	184320
gender_googlenet [26]	-	adience	Face Detection	faces	344576
midas_redweb_diml_movies_megadepth_wsvd_tartanair_hrwsi_apolloscape_blendedmvs_irs_11 [23]	-	redweb, diml, movies, megadepth, wsvd, tartanair, hrwsi, apolloscape, blendedmvs, irs	Depth Estimation	depth	3123200
ssd-10 [28]	-	coco/2017	Object Detection	natural	2175488
ssd_mobilenet_v1_10 [29]	-	coco/2017	Object Detection	natural	209856

Continued on next page

Model ID	Pretraining-Dataset	Training-Dataset	Task	Visual Category	3×3 Filters
super-resolution-10 [30]	-	bsd300	Super Resolution	natural	6432
retinanet-9 [31]	-	imagenet1k	Object Detection	natural	6747136
udnie-9 [22]	-	coco/2014	Style Transfer	natural	184320
version-RFB-320 [32]	-	wider_face/cleaned	Face Detection	faces	7872
version-RFB-640 [32]	-	wider_face	Object Detection	faces	7872
tiny-yolov3-11 [33]	-	coco/2017	Object Detection	natural	928304
pgan_celeba_cropped_disc_11 [34]	-	celeb_a/128_cropped	GAN-Discriminator	faces	2081280
yolov2-coco-9 [35]	-	coco/2014	Object Detection	natural	5458016
pgan_celeba_cropped_gen_11 [34]	-	celeb_a/128_cropped	GAN-Generator	faces	2080768
pgan_celebahq_256_disc_11 [34]	-	celeb_a_hq/256	GAN-Discriminator	faces	2093568
yolov4 [36]	-	coco/2017	Object Detection	natural	5951584
yolov3-10 [33]	-	coco/2017	Object Detection	natural	6189152
tinyyolov2-8 [35]	-	voc/2007, voc/2012	Object Detection	natural	1747504
pgan_celebahq_256_gen_11 [34]	-	celeb_a_hq/256	GAN-Generator	faces	2093056
zfnet512-9 [37]	-	imagenet1k	Classification	natural	655360
pgan_celebahq_512_disc_11 [34]	-	celeb_a_hq/512	GAN-Discriminator	faces	2096640
pgan_celebahq_512_gen_11 [34]	-	celeb_a_hq/512	GAN-Generator	faces	2096128
pgan_dtd_disc_11 [34]	-	dtd	GAN-Discriminator	textures	2081280
pgan_dtd_gen_11 [34]	-	dtd	GAN-Generator	textures	2080768
vgg_ilsvrc_16_age_chalearn_iccv2015 [26]	-	chalearn_lap_2015	Face Detection	faces	1634496
vgg_ilsvrc_16_age_imdb_wiki [26]	-	imdb_wiki	Face Detection	faces	1634496
vgg_ilsvrc_16_gender_imdb_wiki [26]	-	imdb_wiki	Classification	faces	1634496
pytorchencoding_deeplab_resnest50_pcontext_11 [38]	-	voc/2010	Segmentation	natural	3161184
pytorchencoding_deeplab_resnest101_ade_11 [38]	-	ade20k	Segmentation	natural	4284608
arcfaceresnet100-8 [39]	-	refined_ms_celeb_1m	Face Recognition	faces	5783744
pytorchencoding_deeplab_resnest50_ade_11 [38]	-	ade20k	Segmentation	natural	3161184
pytorchencoding_fcn_resnest50_ade_11 [38]	-	ade20k	Segmentation	natural	2571360
pytorchencoding_deeplab_resnest101_pcontext_11 [38]	-	voc/2010	Segmentation	natural	4284608
pytorchencoding_fcn_resnest50_pcontext_11 [38]	-	voc/2010	Segmentation	natural	2571360
pytorchencoding_fcn_resnest50s_ade_11 [38]	-	ade20k	Segmentation	natural	2580672
resnet18_places365_11 [8]	-	places365_small	Classification	natural	1220608
ResNet101-DUC-7 [40]	-	cityscapes/semantic_segmentation	Segmentation	natural	4874432
realesrganx4_custom_11 [41]	-	sberbank_realesrgan	Super Resolution	natural	1853824
resnet50_fractalDB1k_11 [42]	-	fractal_db_1k	Classification	fractals	1257472
robustbench_addepalli2021towards_parn18_corruptions_cifar100_11 [43]	-	cifar100	Classification	natural	1220800
resnet50_fractalDB10k_11 [42]	-	fractal_db_10k	Classification	fractals	1257472
robustbench_addepalli2021towards_parn18_linf_cifar100_11 [43]	-	cifar100	Classification	natural	1220800
resnet50_places365_11 [8]	-	places365_small	Classification	natural	1257472
robustbench_addepalli2021towards_rn18_linf_cifar10_11 [43]	-	cifar10	Classification	natural	1220800
realesrganx8_custom_11 [41]	-	sberbank_realesrgan	Super Resolution	natural	1857920
robustbench_andriushchenko2020understanding_linf_cifar10_11 [44]	-	cifar10	Classification	natural	1220800
robustbench_addepalli2021towards_wrn34_corruptions_cifar100_11 [43]	-	cifar100	Classification	natural	5097008
robustbench_addepalli2021towards_wrn34_linf_cifar100_11 [43]	-	cifar100	Classification	natural	5097008

Continued on next page

Model ID	Pretraining-Dataset	Training-Dataset	Task	Visual Category	3×3 Filters
robustbench_augustin2020adversarial_l2_cifar10_11 [45]	-	cifar10	Classification	natural	1257664
pytorchencoding_deeplab_resnest200_ade_11 [38]	-	ade20k	Segmentation	natural	5464256
robustbench_augustin2020adversarial_34_10_extra_l2_cifar10_11 [45]	-	cifar10	Classification	natural	5097008
pytorchencoding_deeplab_resnest200_pcontext_11 [38]	-	voc/2010	Segmentation	natural	5464256
robustbench_augustin2020adversarial_34_10_l2_cifar10_11 [45]	-	cifar10	Classification	natural	5097008
robustbench_carmon2019unlabeled_linf_cifar10_11 [46]	-	cifar10	Classification	natural	4021808
robustbench_chen2020efficient_linf_cifar100_11 [47]	-	cifar100	Classification	natural	5097008
robustbench_chen2020efficient_linf_cifar10_11 [47]	-	cifar10	Classification	natural	5097008
robustbench_chen2020adversarial_linf_cifar10_11 [48]	-	cifar10	Classification	natural	3772992
robustbench_cui2020learnable_34_10_lbgat6_linf_cifar100_11 [49]	-	cifar100	Classification	natural	5097008
robustbench_cui2020learnable_34_10_linf_cifar10_11 [49]	-	cifar10	Classification	natural	5097008
realesrganx2_custom_11 [41]	-	sberbank_realesrgan	Super Resolution	natural	1854400
robustbench_diffenderfer2021winning_binary_corruptions_cifar100_11 [50]	-	cifar100	Classification	natural	2719936
robustbench_ding2020mma_l2_cifar10_11 [51]	-	cifar10	Classification	natural	644144
robustbench_diffenderfer2021winning_lrr_corruptions_cifar100_11 [50]	-	cifar100	Classification	natural	4882816
robustbench_ding2020mma_linf_cifar10_11 [51]	-	cifar10	Classification	natural	644144
robustbench_engstrom2019robustness_l2_cifar10_11 [52]	-	cifar10	Classification	natural	1257664
pytorchencoding_deeplab_resnest269_ade_11 [38]	-	ade20k	Segmentation	natural	7659712
robustbench_cui2020learnable_34_20_lbgat6_linf_cifar100_11 [49]	-	cifar100	Classification	natural	20382768
robustbench_engstrom2019robustness_linf_cifar10_11 [52]	-	cifar10	Classification	natural	1257664
pytorchencoding_deeplab_resnest269_pcontext_11 [38]	-	voc/2010	Segmentation	natural	7659712
robustbench_engstrom2019robustness_linf_imagenet_11 [52]	-	imagenet1k	Classification	natural	1257472
robustbench_cui2020learnable_34_20_linf_cifar10_11 [49]	-	cifar10	Classification	natural	20382768
robustbench_geirhos2018_sin_corruptions_imagenet_11 [53]	-	imagenet1k	Classification	natural	1257472
robustbench_geirhos2018_sin_in_corruptions_imagenet_11 [53]	-	imagenet1k	Classification	natural	1257472
robustbench_gowal2020uncovering_28_10_extra_linf_cifar10_11 [54]	-	cifar10	Classification	natural	4021808
robustbench_hendrycks2019using_linf_cifar100_11 [55]	-	cifar100	Classification	natural	4021808
robustbench_gowal2020uncovering_34_20_linf_cifar10_11 [54]	-	cifar10	Classification	natural	20382768
robustbench_hendrycks2019using_linf_cifar10_11 [55]	-	cifar10	Classification	natural	4021808
robustbench_gowal2020uncovering_70_16_extra_linf_cifar10_11 [54]	-	cifar10	Classification	natural	29560880
robustbench_hendrycks2020augmix_resnext_corruptions_cifar100_11 [56]	-	cifar100	Classification	natural	258240
robustbench_hendrycks2020augmix_corruptions_imagenet_11 [56]	-	imagenet1k	Classification	natural	1257472
robustbench_gowal2020uncovering_70_16_linf_cifar10_11 [54]	-	cifar10	Classification	natural	29560880
robustbench_hendrycks2020augmix_resnext_corruptions_cifar10_11 [56]	-	cifar10	Classification	natural	258240

Continued on next page

Model ID	Pretraining-Dataset	Training-Dataset	Task	Visual Category	3×3 Filters
robustbench_gowal2020uncovering_extra_l2_cifar10_11 [54]	-	cifar10	Classification	natural	29560880
robustbench_gowal2020uncovering_extra_linf_cifar100_11 [54]	-	cifar100	Classification	natural	29560880
robustbench_hendrycks2020augmix_wrn_corruptions_cifar100_11 [56]	-	cifar100	Classification	natural	247344
robustbench_gowal2020uncovering_l2_cifar10_11 [54]	-	cifar10	Classification	natural	29560880
robustbench_gowal2020uncovering_extra_linf_corruptions_cifar100_11 [54]	-	cifar100	Classification	natural	29560880
robustbench_hendrycks2020augmix_wrn_corruptions_cifar10_11 [56]	-	cifar10	Classification	natural	247344
robustbench_gowal2020uncovering_linf_corruptions_cifar100_11 [54]	-	cifar100	Classification	natural	29560880
robustbench_hendrycks2020many_corruptions_imagenet_11 [57]	-	imagenet1k	Classification	natural	1257472
robustbench_huang2020self_linf_cifar10_11 [58]	-	cifar10	Classification	natural	5097008
robustbench_kireev2021effectiveness_augmixnojsd_corruptions_cifar10_11 [59]	-	cifar10	Classification	natural	1220800
robustbench_kireev2021effectiveness_gauss50percent_corruptions_cifar10_11 [59]	-	cifar10	Classification	natural	1220800
robustbench_kireev2021effectiveness_rlat_corruptions_cifar10_11 [59]	-	cifar10	Classification	natural	1220800
robustbench_huang2021exploring_ema_linf_cifar10_11 [60]	-	cifar10	Classification	natural	7504944
robustbench_kireev2021effectiveness_rlataugmix_corruptions_cifar10_11 [59]	-	cifar10	Classification	natural	1220800
robustbench_huang2021exploring_linf_cifar10_11 [60]	-	cifar10	Classification	natural	7504944
robustbench_kireev2021effectiveness_rlataugmixnojsd_corruptions_cifar10_11 [59]	-	cifar10	Classification	natural	1220800
robustbench_rade2021helper_ddpm_linf_cifar10_11 [61]	-	cifar10	Classification	natural	4021808
robustbench_rade2021helper_extra_linf_cifar10_11 [61]	-	cifar10	Classification	natural	5097008
robustbench_rade2021helper_r18_ddpm_linf_cifar100_11 [61]	-	cifar100	Classification	natural	1392832
robustbench_pang2020boosting_linf_cifar10_11 [62]	-	cifar10	Classification	natural	20382768
robustbench_rade2021helper_r18_ddpm_linf_cifar10_11 [61]	-	cifar10	Classification	natural	1392832
robustbench_rade2021helper_r18_extra_linf_cifar10_11 [61]	-	cifar10	Classification	natural	1392832
robustbench_rebuffi2021fixing_28_10_cutmix_ddpm_l2_cifar10_11 [63]	-	cifar10	Classification	natural	4021808
robustbench_rebuffi2021fixing_28_10_cutmix_ddpm_linf_cifar100_11 [63]	-	cifar100	Classification	natural	4021808
robustbench_rebuffi2021fixing_28_10_cutmix_ddpm_linf_cifar10_11 [63]	-	cifar10	Classification	natural	4021808
robustbench_rebuffi2021fixing_70_16_cutmix_ddpm_l2_cifar10_11 [63]	-	cifar10	Classification	natural	29560880
robustbench_rebuffi2021fixing_106_16_cutmix_ddpm_linf_cifar10_11 [63]	-	cifar10	Classification	natural	46075952
robustbench_rebuffi2021fixing_70_16_cutmix_ddpm_linf_cifar100_11 [63]	-	cifar100	Classification	natural	29560880
robustbench_rebuffi2021fixing_r18_cutmix_ddpm_l2_cifar10_11 [63]	-	cifar10	Classification	natural	1392832
robustbench_rebuffi2021fixing_r18_ddpm_linf_cifar100_11 [63]	-	cifar100	Classification	natural	1392832
robustbench_rebuffi2021fixing_70_16_cutmix_extra_l2_cifar10_11 [63]	-	cifar10	Classification	natural	29560880
robustbench_rebuffi2021fixing_70_16_cutmix_ddpm_linf_cifar10_11 [63]	-	cifar10	Classification	natural	29560880

Continued on next page

Model ID	Pretraining-Dataset	Training-Dataset	Task	Visual Category	3×3 Filters
robustbench_rebuffi2021fixing_70_16_cutmix_extra_linf_cifar10_11 [63]	-	cifar10	Classification	natural	29560880
robustbench_rebuffi2021fixing_r18_ddpm_linf_cifar10_11 [63]	-	cifar10	Classification	natural	1392832
robustbench_rice2020overfitting_l2_cifar10_11 [64]	-	cifar10	Classification	natural	1220800
robustbench_rice2020overfitting_linf_cifar100_11 [64]	-	cifar100	Classification	natural	1220800
robustbench_rony2019decoupling_l2_cifar10_11 [65]	-	cifar10	Classification	natural	4021808
robustbench_salman2020do_50_2_linf_corruptions_imagenet_11 [66]	-	imagenet1k	Classification	natural	5029888
robustbench_rice2020overfitting_linf_cifar10_11 [64]	-	cifar10	Classification	natural	20382768
robustbench_salman2020do_r18_linf_imagenet_11 [66]	-	imagenet1k	Classification	natural	1220608
robustbench_salman2020do_50_2_linf_imagenet_11 [66]	-	imagenet1k	Classification	natural	5029888
robustbench_salman2020do_r50_linf_imagenet_11 [66]	-	imagenet1k	Classification	natural	1257472
robustbench_sehwag2020hydra_linf_cifar10_11 [67]	-	cifar10	Classification	natural	4021808
robustbench_sehwag2021proxy_l2_cifar10_11 [68]	-	cifar10	Classification	natural	5097008
robustbench_sehwag2021proxy_r18_l2_cifar10_11 [68]	-	cifar10	Classification	natural	1220800
robustbench_sehwag2021proxy_linf_cifar10_11 [68]	-	cifar10	Classification	natural	5097008
robustbench_sehwag2021proxy_r18_linf_cifar10_11 [68]	-	cifar10	Classification	natural	1220800
robustbench_sitawarin2020improving_linf_cifar100_11 [69]	-	cifar100	Classification	natural	5097008
robustbench_sitawarin2020improving_linf_cifar10_11 [69]	-	cifar10	Classification	natural	5097008
robustbench_sridhar2021robust_linf_cifar10_11 [70]	-	cifar10	Classification	natural	4021808
robustbench_sridhar2021robust_34_15_linf_cifar10_11 [70]	-	cifar10	Classification	natural	11466288
robustbench_wang2020improving_linf_cifar10_11 [71]	-	cifar10	Classification	natural	4021808
robustbench_wong2020fast_linf_cifar10_11 [72]	-	cifar10	Classification	natural	1220800
robustbench_wong2020fast_linf_imagenet_11 [72]	-	imagenet1k	Classification	natural	1257472
robustbench_wu2020adversarial_extra_linf_cifar10_11 [73]	-	cifar10	Classification	natural	4021808
robustbench_wu2020adversarial_l2_cifar10_11 [73]	-	cifar10	Classification	natural	5097008
robustbench_wu2020adversarial_linf_cifar100_11 [73]	-	cifar100	Classification	natural	5097008
robustbench_wu2020adversarial_linf_cifar10_11 [73]	-	cifar10	Classification	natural	5097008
robustbench_zhang2019theoretically_linf_cifar10_11 [74]	-	cifar10	Classification	natural	5097008
robustbench_zhang2019you_linf_cifar10_11 [75]	-	cifar10	Classification	natural	5097008
robustbench_zhang2020geometry_linf_cifar10_11 [76]	-	cifar10	Classification	natural	4021808
robustbench_zhang2020attacks_linf_cifar10_11 [77]	-	cifar10	Classification	natural	5097008
seismicdeeplearning_dutchf3_hrnet_patch_patch_depth_11 [78]	imagenet1k	dutch_f3	Segmentation	seismic	7165376
seismicdeeplearning_dutchf3_hrnet_patch_section_depth_11 [78]	imagenet1k	dutch_f3	Segmentation	seismic	7165376
seismicdeeplearning_dutchf3_seresnetunet_patch_section_depth_11 [78]	-	dutch_f3	Segmentation	seismic	2760704
starnet_Greyscale_gan_d_prop_9 [79]	-	starnet	GAN-Discriminator	astronomy	196640
stackganv2_imagenet_11 [80]	-	imagenet1k/dog	GAN-Generator	natural	1458256
starnet_RGB_gan_d_prop_9 [79]	-	starnet	GAN-Discriminator	astronomy	196704
seismicdeeplearning_penobscot_hrnet_patch_section_depth_11 [78]	imagenet1k	penobscot	Segmentation	seismic	7165376
stylegan_flickerhq_1024_disc_11 [81]	-	ff_hq/1024	GAN-Discriminator	faces	2097408

Continued on next page

Model ID	Pretraining-Dataset	Training-Dataset	Task	Visual Category	3×3 Filters
timm_adv_inception_v3_imagenet_11 [82]	-	imagenet1k	Classification	natural	632928
taskconditioned_kaist_11 [83]	-	kaist	Object Detection	thermal	6189152
timm_coat_lite_mini_imagenet_11 [84]	-	imagenet1k	Classification	natural	2560
stylegan_flickerhq_1024_gen_11 [81]	-	ff_hq/1024	GAN-Generator	faces	2096896
timm_coat_lite_tiny_imagenet_11 [84]	-	imagenet1k	Classification	natural	1920
timm_cspdarknet53_imagenet_11 [85]	-	imagenet1k	Classification	natural	2412640
timm_coat_lite_small_imagenet_11 [84]	-	imagenet1k	Classification	natural	5200
timm_cspresnet50_imagenet_11 [85]	-	imagenet1k	Classification	natural	1257472
timm_cspresnext50_imagenet_11 [85]	-	imagenet1k	Classification	natural	157184
timm_densenet121_imagenet_11 [12]	-	imagenet1k	Classification	natural	237568
timm_coat_mini_imagenet_11 [84]	-	imagenet1k	Classification	natural	6860
timm_dla102_imagenet_11 [86]	-	imagenet1k	Classification	natural	1712896
timm_coat_tiny_imagenet_11 [84]	-	imagenet1k	Classification	natural	4940
timm_dla102x2_imagenet_11 [86]	-	imagenet1k	Classification	natural	428800
timm_dla102x_imagenet_11 [86]	-	imagenet1k	Classification	natural	214784
timm_dla34_imagenet_11 [86]	-	imagenet1k	Classification	natural	1547008
timm_dla46_c_imagenet_11 [86]	-	imagenet1k	Classification	natural	56064
timm_dla169_imagenet_11 [86]	-	imagenet1k	Classification	natural	2769664
timm_dla46x_c_imagenet_11 [86]	-	imagenet1k	Classification	natural	7680
timm_dla60_imagenet_11 [86]	-	imagenet1k	Classification	natural	1123072
timm_dla60_res2net_imagenet_11 [87]	-	imagenet1k	Classification	natural	645216
timm_dla60_res2next_imagenet_11 [87]	-	imagenet1k	Classification	natural	105984
timm_dla60x_c_imagenet_11 [86]	-	imagenet1k	Classification	natural	9728
timm_dla60x_imagenet_11 [86]	-	imagenet1k	Classification	natural	141056
timm_dpn68_imagenet_11 [88]	-	imagenet1k	Classification	natural	206366
timm_dpn68b_imagenet_11 [88]	-	imagenet1k	Classification	natural	206366
timm_dpn107_imagenet_11 [88]	-	imagenet1k	Classification	natural	438400
timm_dpn92_imagenet_11 [88]	-	imagenet1k	Classification	natural	152928
timm_dpn131_imagenet_11 [88]	-	imagenet1k	Classification	natural	432640
timm_ecaresnet101d_pruned_imagenet_11 [89]	-	imagenet1k	Classification	natural	1623471
timm_dpn98_imagenet_11 [88]	-	imagenet1k	Classification	natural	344960
timm_ecaresnet101d_imagenet_11 [89]	-	imagenet1k	Classification	natural	2374752
timm_ecaresnet26t_imagenet_11 [89]	-	imagenet1k	Classification	natural	699208
timm_ecaresnet50d_imagenet_11 [89]	-	imagenet1k	Classification	natural	1260640
timm_ecaresnet50d_pruned_imagenet_11 [89]	-	imagenet1k	Classification	natural	985657
timm_ecaresnet50t_imagenet_11 [89]	-	imagenet1k	Classification	natural	1260360
timm_efficientnet_b0_imagenet_11 [24]	-	imagenet1k	Classification	natural	2720
timm_ecaresnetlight_imagenet_11 [89]	-	imagenet1k	Classification	natural	1527808
timm_efficientnet_b1_imagenet_11 [24]	-	imagenet1k	Classification	natural	5280
timm_efficientnet_b2_imagenet_11 [24]	-	imagenet1k	Classification	natural	5760
timm_efficientnet_b1_pruned_imagenet_11 [24]	-	imagenet1k	Classification	natural	4030
timm_efficientnet_b2_pruned_imagenet_11 [24]	-	imagenet1k	Classification	natural	4753
timm_efficientnet_b3_imagenet_11 [24]	-	imagenet1k	Classification	natural	7000
timm_efficientnet_b3_pruned_imagenet_11 [24]	-	imagenet1k	Classification	natural	5186
timm_efficientnet_b4_imagenet_11 [24]	-	imagenet1k	Classification	natural	8952
timm_efficientnet_el_imagenet_11 [90]	-	imagenet1k	Classification	natural	181368
timm_efficientnet_el_pruned_imagenet_11 [90]	-	imagenet1k	Classification	natural	181368
timm_efficientnet_em_imagenet_11 [90]	-	imagenet1k	Classification	natural	108384
timm_efficientnet_es_imagenet_11 [90]	-	imagenet1k	Classification	natural	79456
timm_efficientnet_es_pruned_imagenet_11 [90]	-	imagenet1k	Classification	natural	79456
timm_efficientnet_lite0_imagenet_11 [24]	-	imagenet1k	Classification	natural	2720
timm_ecaresnet269d_imagenet_11 [89]	-	imagenet1k	Classification	natural	5749856
timm_ese_vovnet19b_dw_imagenet_11 [91]	-	imagenet1k	Classification	natural	2432
timm_efficientnetv2_rw_s_imagenet_11 [92]	-	imagenet1k	Classification	natural	124616
timm_ese_vovnet39b_imagenet_11 [91]	-	imagenet1k	Classification	natural	1581248
timm_fbnetc_100_imagenet_11 [93]	-	imagenet1k	Classification	natural	1504
timm_ens_adv_inception_resnet_v2_imagenet_11 [94]	-	imagenet1k	Classification	natural	714848
timm_gernet_l_imagenet_11 [95]	-	imagenet1k	Classification	natural	326624
timm_efficientnetv2_rw_m_imagenet_11 [92]	-	imagenet1k	Classification	natural	240416
timm_gernet_m_imagenet_11 [95]	-	imagenet1k	Classification	natural	318944
timm_gernet_s_imagenet_11 [95]	-	imagenet1k	Classification	natural	85431
timm_ghostnet_100_imagenet_11 [9]	-	imagenet1k	Classification	natural	4616

Continued on next page

Model ID	Pretraining-Dataset	Training-Dataset	Task	Visual Category	3×3 Filters
timm_gluon_inception_v3_imagenet_11 [96]	-	imagenet1k	Classification	natural	632928
timm_gluon_resnet101_v1b_imagenet_11 [96]	-	imagenet1k	Classification	natural	2371584
timm_gluon_resnet101_v1d_imagenet_11 [96]	-	imagenet1k	Classification	natural	2374752
timm_gluon_resnet101_v1c_imagenet_11 [96]	-	imagenet1k	Classification	natural	2374752
timm_gluon_resnet101_v1s_imagenet_11 [96]	-	imagenet1k	Classification	natural	2384064
timm_gluon_resnet18_v1b_imagenet_11 [96]	-	imagenet1k	Classification	natural	1220608
timm_gluon_resnet34_v1b_imagenet_11 [96]	-	imagenet1k	Classification	natural	2342912
timm_gluon_resnet152_v1b_imagenet_11 [96]	-	imagenet1k	Classification	natural	3289088
timm_gluon_resnet50_v1b_imagenet_11 [96]	-	imagenet1k	Classification	natural	1257472
timm_gluon_resnet152_v1s_imagenet_11 [96]	-	imagenet1k	Classification	natural	3301568
timm_gluon_resnet50_v1d_imagenet_11 [96]	-	imagenet1k	Classification	natural	1260640
timm_gluon_resnet50_v1c_imagenet_11 [96]	-	imagenet1k	Classification	natural	1260640
timm_gluon_resnet152_v1d_imagenet_11 [96]	-	imagenet1k	Classification	natural	3292256
timm_gluon_resnet152_v1c_imagenet_11 [96]	-	imagenet1k	Classification	natural	3292256
timm_gluon_resnet50_v1s_imagenet_11 [96]	-	imagenet1k	Classification	natural	1269952
timm_gluon_resnext50_32x4d_imagenet_11 [96]	-	imagenet1k	Classification	natural	157184
timm_gluon_resnext101_32x4d_imagenet_11 [96]	-	imagenet1k	Classification	natural	296448
timm_gluon_seresnext50_32x4d_imagenet_11 [96]	-	imagenet1k	Classification	natural	157184
timm_gluon_seresnext101_32x4d_imagenet_11 [96]	-	imagenet1k	Classification	natural	296448
timm_gluon_resnext101_64x4d_imagenet_11 [96]	-	imagenet1k	Classification	natural	592896
timm_hardcorenas_a_imagenet_11 [97]	-	imagenet1k	Classification	natural	128
timm_gluon_seresnext101_64x4d_imagenet_11 [96]	-	imagenet1k	Classification	natural	592896
timm_hardcorenas_b_imagenet_11 [97]	-	imagenet1k	Classification	natural	2264
timm_hardcorenas_c_imagenet_11 [97]	-	imagenet1k	Classification	natural	2192
timm_gluon_xception65_imagenet_11 [96]	-	imagenet1k	Classification	natural	46336
timm_hardcorenas_d_imagenet_11 [97]	-	imagenet1k	Classification	natural	2776
timm_gluon_senet154_imagenet_11 [96]	-	imagenet1k	Classification	natural	3176128
timm_hardcorenas_e_imagenet_11 [97]	-	imagenet1k	Classification	natural	1880
timm_hardcorenas_f_imagenet_11 [97]	-	imagenet1k	Classification	natural	3728
timm_hrnet_w18_small_imagenet_11 [98]	-	imagenet1k	Classification	natural	934592
timm_hrnet_w18_imagenet_11 [98]	-	imagenet1k	Classification	natural	1809204
timm_hrnet_w18_small_v2_imagenet_11 [98]	-	imagenet1k	Classification	natural	1188004
timm_hrnet_w30_imagenet_11 [98]	-	imagenet1k	Classification	natural	3595380
timm_hrnet_w32_imagenet_11 [98]	-	imagenet1k	Classification	natural	3979456
timm_hrnet_w40_imagenet_11 [98]	-	imagenet1k	Classification	natural	5762560
timm_hrnet_w44_imagenet_11 [98]	-	imagenet1k	Classification	natural	6802192
timm_hrnet_w48_imagenet_11 [98]	-	imagenet1k	Classification	natural	7940544
timm_inception_resnet_v2_imagenet_11 [94]	-	imagenet1k	Classification	natural	714848
timm_inception_v4_imagenet_11 [94]	-	imagenet1k	Classification	natural	531552
timm_legacy_seresnet101_imagenet_11 [99]	-	imagenet1k	Classification	natural	2371584
timm_hrnet_w64_imagenet_11 [98]	-	imagenet1k	Classification	natural	13481152
timm_legacy_seresnet18_imagenet_11 [99]	-	imagenet1k	Classification	natural	1220608
timm_legacy_seresnet34_imagenet_11 [99]	-	imagenet1k	Classification	natural	2342912
timm_legacy_senet154_imagenet_11 [99]	-	imagenet1k	Classification	natural	3176128
timm_legacy_seresnet152_imagenet_11 [99]	-	imagenet1k	Classification	natural	3289088
timm_legacy_seresnet50_imagenet_11 [99]	-	imagenet1k	Classification	natural	1257472
timm_legacy_seresnext26_32x4d_imagenet_11 [99]	-	imagenet1k	Classification	natural	87040
timm_legacy_seresnext101_32x4d_imagenet_11 [99]	-	imagenet1k	Classification	natural	296448
timm_legacy_seresnext50_32x4d_imagenet_11 [99]	-	imagenet1k	Classification	natural	157184
timm_mixnet_l_imagenet_11 [100]	-	imagenet1k	Classification	natural	3868
timm_mixnet_m_imagenet_11 [100]	-	imagenet1k	Classification	natural	2918
timm_mixnet_s_imagenet_11 [100]	-	imagenet1k	Classification	natural	2284
timm_mixnet_xl_imagenet_11 [100]	-	imagenet1k	Classification	natural	5672
timm_mnasnet_100_imagenet_11 [101]	-	imagenet1k	Classification	natural	2528
timm_mobilenetv2_100_imagenet_11 [16]	-	imagenet1k	Classification	natural	7232
timm_mobilenetv2_110d_imagenet_11 [16]	-	imagenet1k	Classification	natural	10304
timm_mobilenetv2_120d_imagenet_11 [16]	-	imagenet1k	Classification	natural	14048
timm_mobilenetv2_140_imagenet_11 [16]	-	imagenet1k	Classification	natural	10176
timm_mobilenetv3_large_100_imagenet_11 [102]	-	imagenet1k	Classification	natural	2160
timm_mobilenetv3_large_100_miil_imagenet_11 [102]	imagenet21k	imagenet1k	Classification	natural	2160
timm_mobilenetv3_large_100_miil_in21k_imagenet21k_p_11 [102]	-	imagenet21k_p	Classification	natural	2160

Continued on next page

Model ID	Pretraining-Dataset	Training-Dataset	Task	Visual Category	3×3 Filters
timm_mobilenetv3_rw_imagenet_11 [102]	-	imagenet1k	Classification	natural	2160
timm_pit_s_224_imagenet_11 [103]	-	imagenet1k	Classification	natural	864
timm_pit_b_224_imagenet_11 [103]	-	imagenet1k	Classification	natural	1536
timm_pit_b_distilled_224_imagenet_11 [103]	-	imagenet1k	Classification	natural	1536
timm_pit_s_distilled_224_imagenet_11 [103]	-	imagenet1k	Classification	natural	864
timm_nasnetalarge_imagenet_11 [104]	-	imagenet1k	Classification	natural	44892
timm_pit_ti_224_imagenet_11 [103]	-	imagenet1k	Classification	natural	384
timm_pit_ti_distilled_224_imagenet_11 [103]	-	imagenet1k	Classification	natural	384
timm_pit_xs_224_imagenet_11 [103]	-	imagenet1k	Classification	natural	576
timm_pit_xs_distilled_224_imagenet_11 [103]	-	imagenet1k	Classification	natural	576
timm_regnetx_002_imagenet_11 [105]	-	imagenet1k	Classification	natural	26208
timm_pnasnet5large_imagenet_11 [106]	-	imagenet1k	Classification	natural	37590
timm_regnetx_004_imagenet_11 [105]	-	imagenet1k	Classification	natural	94304
timm_regnetx_006_imagenet_11 [105]	-	imagenet1k	Classification	natural	125664
timm_regnetx_008_imagenet_11 [105]	-	imagenet1k	Classification	natural	93280
timm_regnetx_016_imagenet_11 [105]	-	imagenet1k	Classification	natural	161376
timm_regnetx_032_imagenet_11 [105]	-	imagenet1k	Classification	natural	472416
timm_regnetx_040_imagenet_11 [105]	-	imagenet1k	Classification	natural	476896
timm_regnetx_064_imagenet_11 [105]	-	imagenet1k	Classification	natural	636704
timm_regnety_002_imagenet_11 [105]	-	imagenet1k	Classification	natural	26208
timm_regnety_004_imagenet_11 [105]	-	imagenet1k	Classification	natural	34080
timm_regnety_006_imagenet_11 [105]	-	imagenet1k	Classification	natural	73824
timm_regnetx_120_imagenet_11 [105]	-	imagenet1k	Classification	natural	1655904
timm_regnety_008_imagenet_11 [105]	-	imagenet1k	Classification	natural	72800
timm_regnetx_080_imagenet_11 [105]	-	imagenet1k	Classification	natural	1683296
timm_regnety_016_imagenet_11 [105]	-	imagenet1k	Classification	natural	199392
timm_regnety_032_imagenet_11 [105]	-	imagenet1k	Classification	natural	245472
timm_repvgg_b0_imagenet_11 [107]	-	imagenet1k	Classification	natural	1450176
timm_regnety_040_imagenet_11 [105]	-	imagenet1k	Classification	natural	622688
timm_regnety_064_imagenet_11 [105]	-	imagenet1k	Classification	natural	933216
timm_regnetx_160_imagenet_11 [105]	-	imagenet1k	Classification	natural	2211936
timm_repvgg_a2_imagenet_11 [107]	-	imagenet1k	Classification	natural	2675904
timm_regnety_120_imagenet_11 [105]	-	imagenet1k	Classification	natural	1655904
timm_regnety_080_imagenet_11 [105]	-	imagenet1k	Classification	natural	733920
timm_repvgg_b1_imagenet_11 [107]	-	imagenet1k	Classification	natural	5529792
timm_repvgg_b1g4_imagenet_11 [107]	-	imagenet1k	Classification	natural	3784896
timm_regnetx_320_imagenet_11 [105]	-	imagenet1k	Classification	natural	4261920
timm_regnety_160_imagenet_11 [105]	-	imagenet1k	Classification	natural	2107488
timm_repvgg_b2g4_imagenet_11 [107]	-	imagenet1k	Classification	natural	5911232
timm_res2net101_26w_4s_imagenet_11 [87]	-	imagenet1k	Classification	natural	1174212
timm_repvgg_b3g4_imagenet_11 [107]	-	imagenet1k	Classification	natural	8116416
timm_res2net50_26w_4s_imagenet_11 [87]	-	imagenet1k	Classification	natural	622596
timm_repvgg_b2_imagenet_11 [107]	-	imagenet1k	Classification	natural	8637632
timm_res2net50_26w_6s_imagenet_11 [87]	-	imagenet1k	Classification	natural	1037660
timm_regnety_320_imagenet_11 [105]	-	imagenet1k	Classification	natural	5651616
timm_res2net50_48w_2s_imagenet_11 [87]	-	imagenet1k	Classification	natural	707328
timm_res2net50_14w_8s_imagenet_11 [87]	-	imagenet1k	Classification	natural	421204
timm_res2net50_26w_8s_imagenet_11 [87]	-	imagenet1k	Classification	natural	1452724
timm_res2next50_imagenet_11 [87]	-	imagenet1k	Classification	natural	117888
timm_resnest14d_imagenet_11 [38]	-	imagenet1k	Classification	natural	351328
timm_repvgg_b3_imagenet_11 [107]	-	imagenet1k	Classification	natural	12042432
timm_resnest26d_imagenet_11 [38]	-	imagenet1k	Classification	natural	699488
timm_resnest50d_1s4x24d_imagenet_11 [38]	-	imagenet1k	Classification	natural	710496
timm_resnest101e_imagenet_11 [38]	-	imagenet1k	Classification	natural	2384064
timm_resnest50d_4s2x40d_imagenet_11 [38]	-	imagenet1k	Classification	natural	985568
timm_resnest50d_imagenet_11 [38]	-	imagenet1k	Classification	natural	1260640
timm_resnet18d_imagenet_11 [18]	-	imagenet1k	Classification	natural	1223776
timm_resnet101d_imagenet_11 [18]	-	imagenet1k	Classification	natural	2374752
timm_resnest200e_imagenet_11 [38]	-	imagenet1k	Classification	natural	3563712
timm_resnet152d_imagenet_11 [18]	-	imagenet1k	Classification	natural	3292256
timm_resnet200d_imagenet_11 [18]	-	imagenet1k	Classification	natural	3554400
timm_resnet26_imagenet_11 [18]	-	imagenet1k	Classification	natural	696320

Continued on next page

Model ID	Pretraining-Dataset	Training-Dataset	Task	Visual Category	3×3 Filters
timm_resnet26d_imagenet_11 [18]	-	imagenet1k	Classification	natural	699488
timm_resnet34_imagenet_11 [18]	-	imagenet1k	Classification	natural	2342912
timm_resnet34d_imagenet_11 [18]	-	imagenet1k	Classification	natural	2346080
timm_resnest269e_imagenet_11 [38]	-	imagenet1k	Classification	natural	5759168
timm_resnet50_imagenet_11 [18]	-	imagenet1k	Classification	natural	1257472
timm_resnet50d_imagenet_11 [18]	-	imagenet1k	Classification	natural	1260640
timm_resnet51q_imagenet_11 [18]	-	imagenet1k	Classification	natural	111152
timm_resnetrs101_imagenet_11 [108]	-	imagenet1k	Classification	natural	2378848
timm_resnetrs152_imagenet_11 [108]	-	imagenet1k	Classification	natural	3296352
timm_resnetrs200_imagenet_11 [108]	-	imagenet1k	Classification	natural	3558496
timm_resnetrs50_imagenet_11 [108]	-	imagenet1k	Classification	natural	1264736
timm_resnext50_32x4d_imagenet_11 [109]	-	imagenet1k	Classification	natural	157184
timm_resnetrs270_imagenet_11 [108]	-	imagenet1k	Classification	natural	5020768
timm_resnext50d_32x4d_imagenet_11 [109]	-	imagenet1k	Classification	natural	160352
timm_rexnet_100_imagenet_11 [110]	-	imagenet1k	Classification	natural	8654
timm_rexnet_130_imagenet_11 [110]	-	imagenet1k	Classification	natural	11256
timm_rexnet_150_imagenet_11 [110]	-	imagenet1k	Classification	natural	12984
timm_rexnet_200_imagenet_11 [110]	-	imagenet1k	Classification	natural	17308
timm_selecsls42b_imagenet_11 [111]	-	imagenet1k	Classification	natural	3214432
timm_resnetrs350_imagenet_11 [108]	-	imagenet1k	Classification	natural	6380640
timm_selecsls60_imagenet_11 [111]	-	imagenet1k	Classification	natural	2913504
timm_selecsls60b_imagenet_11 [111]	-	imagenet1k	Classification	natural	3175648
timm_semnasnet_100_imagenet_11 [101]	-	imagenet1k	Classification	natural	4160
timm_seresnet50_imagenet_11 [99]	-	imagenet1k	Classification	natural	1257472
timm_seresnext26d_32x4d_imagenet_11 [99]	-	imagenet1k	Classification	natural	90208
timm_resnetrs420_imagenet_11 [108]	-	imagenet1k	Classification	natural	7494752
timm_seresnext26t_32x4d_imagenet_11 [99]	-	imagenet1k	Classification	natural	89928
timm_seresnet152d_imagenet_11 [99]	-	imagenet1k	Classification	natural	3292256
timm_seresnext50_32x4d_imagenet_11 [99]	-	imagenet1k	Classification	natural	157184
timm_skresnet18_imagenet_11 [112]	-	imagenet1k	Classification	natural	1220608
timm_skresnet34_imagenet_11 [112]	-	imagenet1k	Classification	natural	2342912
timm_spnasnet_100_imagenet_11 [113]	-	imagenet1k	Classification	natural	2552
timm_skresnext50_32x4d_imagenet_11 [112]	-	imagenet1k	Classification	natural	314368
timm_ssl_resnet18_imagenet_11 [114]	yfcc100m	imagenet1k	Classification	natural	1220608
timm_ssl_resnet50_imagenet_11 [114]	yfcc100m	imagenet1k	Classification	natural	1257472
timm_ssl_resnext50_32x4d_imagenet_11 [114]	yfcc100m	imagenet1k	Classification	natural	157184
timm_ssl_resnext101_32x4d_imagenet_11 [114]	yfcc100m	imagenet1k	Classification	natural	296448
timm_swsl_resnet18_imagenet_11 [114]	instagram1b	imagenet1k	Classification	natural	1220608
timm_ssl_resnext101_32x8d_imagenet_11 [114]	yfcc100m	imagenet1k	Classification	natural	1185792
timm_swsl_resnet50_imagenet_11 [114]	instagram1b	imagenet1k	Classification	natural	1257472
timm_ssl_resnext101_32x16d_imagenet_11 [114]	yfcc100m	imagenet1k	Classification	natural	4743168
timm_swsl_resnext101_32x4d_imagenet_11 [114]	instagram1b	imagenet1k	Classification	natural	296448
timm_swsl_resnext50_32x4d_imagenet_11 [114]	instagram1b	imagenet1k	Classification	natural	157184
timm_swsl_resnext101_32x8d_imagenet_11 [114]	instagram1b	imagenet1k	Classification	natural	1185792
timm_tf_efficientnet_b0_ap_imagenet_11 [115]	-	imagenet1k	Classification	natural	2720
timm_tf_efficientnet_b0_imagenet_11 [24]	-	imagenet1k	Classification	natural	2720
timm_tf_efficientnet_b0_ns_imagenet_11 [116]	jft300m	imagenet1k	Classification	natural	2720
timm_tf_efficientnet_b1_ap_imagenet_11 [115]	-	imagenet1k	Classification	natural	5280
timm_tf_efficientnet_b1_imagenet_11 [24]	-	imagenet1k	Classification	natural	5280
timm_swsl_resnext101_32x16d_imagenet_11 [114]	instagram1b	imagenet1k	Classification	natural	4743168
timm_tf_efficientnet_b1_ns_imagenet_11 [116]	jft300m	imagenet1k	Classification	natural	5280
timm_tf_efficientnet_b2_ap_imagenet_11 [115]	-	imagenet1k	Classification	natural	5760
timm_tf_efficientnet_b2_imagenet_11 [24]	-	imagenet1k	Classification	natural	5760
timm_tf_efficientnet_b2_ns_imagenet_11 [116]	jft300m	imagenet1k	Classification	natural	5760
timm_tf_efficientnet_b3_ap_imagenet_11 [115]	-	imagenet1k	Classification	natural	7000
timm_tf_efficientnet_b3_imagenet_11 [24]	-	imagenet1k	Classification	natural	7000
timm_tf_efficientnet_b3_ns_imagenet_11 [116]	jft300m	imagenet1k	Classification	natural	7000
timm_tf_efficientnet_b4_ap_imagenet_11 [115]	-	imagenet1k	Classification	natural	8952
timm_tf_efficientnet_b4_imagenet_11 [24]	-	imagenet1k	Classification	natural	8952
timm_tf_efficientnet_b4_ns_imagenet_11 [116]	jft300m	imagenet1k	Classification	natural	8952
timm_tf_efficientnet_b5_ap_imagenet_11 [115]	-	imagenet1k	Classification	natural	14304
timm_tf_efficientnet_b5_imagenet_11 [24]	-	imagenet1k	Classification	natural	14304

Continued on next page

Model ID	Pretraining-Dataset	Training-Dataset	Task	Visual Category	3×3 Filters
timm_tf_efficientnet_b5_ns_imagenet_11 [116]	jft300m	imagenet1k	Classification	natural	14304
timm_tf_efficientnet_b6_ap_imagenet_11 [115]	-	imagenet1k	Classification	natural	17136
timm_tf_efficientnet_b6_imagenet_11 [24]	-	imagenet1k	Classification	natural	17136
timm_tf_efficientnet_b6_ns_imagenet_11 [116]	jft300m	imagenet1k	Classification	natural	17136
timm_tf_efficientnet_b7_ap_imagenet_11 [115]	-	imagenet1k	Classification	natural	25216
timm_tf_efficientnet_el_imagenet_11 [90]	-	imagenet1k	Classification	natural	181368
timm_tf_efficientnet_b7_imagenet_11 [24]	-	imagenet1k	Classification	natural	25216
timm_tf_efficientnet_b7_ns_imagenet_11 [116]	jft300m	imagenet1k	Classification	natural	25216
timm_tf_efficientnet_b8_ap_imagenet_11 [115]	-	imagenet1k	Classification	natural	29232
timm_tf_efficientnet_em_imagenet_11 [90]	-	imagenet1k	Classification	natural	108384
timm_tf_efficientnet_b8_imagenet_11 [24]	-	imagenet1k	Classification	natural	29232
timm_tf_efficientnet_es_imagenet_11 [90]	-	imagenet1k	Classification	natural	79456
timm_tf_efficientnet_lite0_imagenet_11 [24]	-	imagenet1k	Classification	natural	2720
timm_tf_efficientnet_lite1_imagenet_11 [24]	-	imagenet1k	Classification	natural	3344
timm_tf_efficientnet_lite2_imagenet_11 [24]	-	imagenet1k	Classification	natural	3632
timm_tf_efficientnet_lite3_imagenet_11 [24]	-	imagenet1k	Classification	natural	4640
timm_tf_efficientnet_lite4_imagenet_11 [24]	-	imagenet1k	Classification	natural	6176
timm_tf_efficientnetv2_b0_imagenet_11 [92]	-	imagenet1k	Classification	natural	32000
timm_tf_efficientnetv2_b1_imagenet_11 [92]	-	imagenet1k	Classification	natural	47776
timm_tf_efficientnetv2_b2_imagenet_11 [92]	-	imagenet1k	Classification	natural	56912
timm_tf_efficientnetv2_b3_imagenet_11 [92]	-	imagenet1k	Classification	natural	70040
timm_tf_efficientnetv2_s_imagenet_11 [92]	-	imagenet1k	Classification	natural	123272
timm_tf_efficientnetv2_m_imagenet_11 [92]	-	imagenet1k	Classification	natural	217608
timm_tf_efficientnetv2_m_in21ft1k_imagenet_11 [92]	imagenet21k	imagenet1k	Classification	natural	217608
timm_tf_efficientnetv2_s_in21ft1k_imagenet_11 [92]	imagenet21k	imagenet1k	Classification	natural	123272
timm_tf_efficientnetv2_m_in21k_imagenet21k_e_11 [92]	-	imagenet21k_e	Classification	natural	217608
timm_tf_inception_v3_imagenet_11 [17]	-	imagenet1k	Classification	natural	632928
timm_tf_efficientnetv2_s_in21k_imagenet21k_e_11 [92]	-	imagenet21k_e	Classification	natural	123272
timm_tf_mixnet_l_imagenet_11 [100]	-	imagenet1k	Classification	natural	3868
timm_tf_efficientnetv2_l_imagenet_11 [92]	-	imagenet1k	Classification	natural	458784
timm_tf_mixnet_m_imagenet_11 [100]	-	imagenet1k	Classification	natural	2918
timm_tf_efficientnetv2_l_in21ft1k_imagenet_11 [92]	imagenet21k	imagenet1k	Classification	natural	458784
timm_tf_efficientnetv2_l_in21k_imagenet21k_e_11 [92]	-	imagenet21k_e	Classification	natural	458784
timm_tf_mixnet_s_imagenet_11 [100]	-	imagenet1k	Classification	natural	2284
timm_tf_mobilenetv3_large_075_imagenet_11 [102]	-	imagenet1k	Classification	natural	1752
timm_tf_mobilenetv3_large_100_imagenet_11 [102]	-	imagenet1k	Classification	natural	2160
timm_tf_mobilenetv3_large_minimal_100_imagenet_11 [102]	-	imagenet1k	Classification	natural	5064
timm_tf_mobilenetv3_small_075_imagenet_11 [102]	-	imagenet1k	Classification	natural	224
timm_tf_mobilenetv3_small_100_imagenet_11 [102]	-	imagenet1k	Classification	natural	224
timm_tf_mobilenetv3_small_minimal_100_imagenet_11 [102]	-	imagenet1k	Classification	natural	2504
timm_tf_efficientnet_l2_ns_475_imagenet_11 [116]	jft300m	imagenet1k	Classification	natural	85816
timm_xception41_imagenet_11 [117]	-	imagenet1k	Classification	natural	28864
timm_xception65_imagenet_11 [117]	-	imagenet1k	Classification	natural	46336
timm_visformer_small_imagenet_11 [118]	-	imagenet1k	Classification	natural	129024
timm_xception_imagenet_11 [117]	-	imagenet1k	Classification	natural	25192
timm_tf_efficientnet_l2_ns_imagenet_11 [116]	jft300m	imagenet1k	Classification	natural	85816
timm_xception71_imagenet_11 [117]	-	imagenet1k	Classification	natural	49288
tinynet_a_imagenet_11 [119]	-	imagenet1k	Classification	natural	3200
timm_wide_resnet50_2_imagenet_11 [120]	-	imagenet1k	Classification	natural	5029888
timm_twins_pcpvt_small_imagenet_11 [121]	-	imagenet1k	Classification	natural	1024
tinynet_b_imagenet_11 [119]	-	imagenet1k	Classification	natural	2192
tinynet_c_imagenet_11 [119]	-	imagenet1k	Classification	natural	1520
timm_twins_svt_small_imagenet_11 [121]	-	imagenet1k	Classification	natural	960
tinynet_d_imagenet_11 [119]	-	imagenet1k	Classification	natural	1184
tinynet_e_imagenet_11 [119]	-	imagenet1k	Classification	natural	1136
timm_twins_svt_base_imagenet_11 [121]	-	imagenet1k	Classification	natural	1440
timm_twins_pcpvt_base_imagenet_11 [121]	-	imagenet1k	Classification	natural	1024

Continued on next page

Model ID	Pretraining-Dataset	Training-Dataset	Task	Visual Category	3×3 Filters
torchseg_dfn_R101_v1c_voc_11 [122]	-	voc/2012	Segmentation	natural	6649810
torchseg_pspnet_R101_v1c_ade_11 [123]	-	ade20k	Segmentation	natural	4481216
alexnet_imagenet_11 [11]	-	imagenet1k	Classification	natural	237568
densenet121_imagenet_11 [12]	-	imagenet1k	Classification	natural	237568
timm_twins_svt_large_imagenet_11 [121]	-	imagenet1k	Classification	natural	1920
densenet161_imagenet_11 [12]	-	imagenet1k	Classification	natural	718848
densenet169_imagenet_11 [12]	-	imagenet1k	Classification	natural	335872
googlenet_imagenet_11 [14]	-	imagenet1k	Classification	natural	368384
mnasnet0_5_imagenet_11 [101]	-	imagenet1k	Classification	natural	1288
mobilenet_v2_imagenet_11 [16]	-	imagenet1k	Classification	natural	7232
mnasnet1_0_imagenet_11 [101]	-	imagenet1k	Classification	natural	2528
densenet201_imagenet_11 [12]	-	imagenet1k	Classification	natural	401408
inception_v3_imagenet_11 [17]	-	imagenet1k	Classification	natural	632928
resnet101_imagenet_11 [18]	-	imagenet1k	Classification	natural	2371584
timm_twins_pcpvt_large_imagenet_11 [121]	-	imagenet1k	Classification	natural	1024
resnet152_imagenet_11 [18]	-	imagenet1k	Classification	natural	3289088
resnet18_imagenet_11 [18]	-	imagenet1k	Classification	natural	1220608
resnet34_imagenet_11 [18]	-	imagenet1k	Classification	natural	2342912
resnet50_imagenet_11 [18]	-	imagenet1k	Classification	natural	1257472
resnext101_32x8d_imagenet_11 [109]	-	imagenet1k	Classification	natural	1185792
resnext50_32x4d_imagenet_11 [109]	-	imagenet1k	Classification	natural	157184
shufflenet_v2_x0_5_imagenet_11 [124]	-	imagenet1k	Classification	natural	1104
shufflenet_v2_x1_0_imagenet_11 [124]	-	imagenet1k	Classification	natural	2532
squeezenet1_0_imagenet_11 [125]	-	imagenet1k	Classification	natural	61440
squeezenet1_1_imagenet_11 [125]	-	imagenet1k	Classification	natural	61632
vgg11_bn_imagenet_11 [19]	-	imagenet1k	Classification	natural	1024192
vgg16_bn_imagenet_11 [19]	-	imagenet1k	Classification	natural	1634496
vgg13_imagenet_11 [19]	-	imagenet1k	Classification	natural	1044672
vgg11_imagenet_11 [19]	-	imagenet1k	Classification	natural	1024192
vgg13_bn_imagenet_11 [19]	-	imagenet1k	Classification	natural	1044672
vgg16_imagenet_11 [19]	-	imagenet1k	Classification	natural	1634496
vgg19_bn_imagenet_11 [19]	-	imagenet1k	Classification	natural	2224320
torchxrayvision_densenet121_all_11 [126]	-	kaggle/rsna_pneumonia_detection_challenge, nih_chest_x_ray8, padchest, chexpert, mimic_cxr/v1.0.0_small	Classification	medical xray	237568
vgg19_imagenet_11 [19]	-	imagenet1k	Classification	natural	2224320
torchxrayvision_densenet121_chex_11 [126]	-	chexpert	Classification	medical xray	237568
wide_resnet50_2_imagenet_11 [120]	-	imagenet1k	Classification	natural	5029888
torchxrayvision_densenet121_kaggle_11 [126]	-	kaggle/rsna_pneumonia_detection_challenge	Classification	medical xray	237568
torchxrayvision_densenet121_mimic_ch_11 [126]	-	mimic_cxr/v1.0.0_small	Classification	medical xray	237568
torchxrayvision_densenet121_mimic_nb_11 [126]	-	mimic_cxr/v1.0.0_small	Classification	medical xray	237568
torchxrayvision_densenet121_nih_11 [126]	-	nih_chest_x_ray8	Classification	medical xray	237568
torchxrayvision_densenet121_pc_11 [126]	-	padchest	Classification	medical xray	237568

Continued on next page

Model ID	**Pretraining-Dataset**	**Training-Dataset**	**Task**	**Visual Category**	3×3 **Filters**
torchxrayvision_resnet50_512_all_11 [126]	-	kaggle/rsna_pneumonia_detection_challenge, nih_chest_x_ray8, padchest, chexpert, mimic_cxr/v1.0.0_small	Classification	medical xray	1257472
torchxrayvision_resnet101_elastic_ae_padchest_nih_chexpert_mimic_nb_mimic_ch_11 [126]	-	padchest, nih_chest_x_ray8, chexpert, mimic_cxr/v1.0.0_small	Auto-Encoder	medical xray	1728000
wide_resnet101_2_imagenet_11 [120]	-	imagenet1k	Classification	natural	9486336
unet_carvana_carvana_11 [127]	-	kaggle/carvana_image_masking_challenge	Segmentation	cars	1917120
unet_lgg_mri_segmentation_11 [127]	-	kaggle/lgg_mri_segmentation	Segmentation	medical mri	784480
yolov5s_v40_coco2017_12 [128]	-	coco/2017	Object Detection	natural	486784
yolov5m_v40_coco2017_12 [128]	-	coco/2017	Object Detection	natural	1613376
yolov5l_v40_coco2017_12 [128]	-	coco/2017	Object Detection	natural	3789568
yolov5x_v40_coco2017_12 [128]	-	coco/2017	Object Detection	natural	7360960

References

[1] Tommy Odland, "tommyod/kdepy: Kernel density estimation in python," 2018. 2

[2] Huy Phan, "huyvnphan/pytorch_cifar10," Jan. 2021. 3, 19

[3] Ross Wightman, "Pytorch image models." https://github.com/rwightman/pytorch-image-models, 2019. 19

[4] Francesco Croce, Maksym Andriushchenko, Vikash Sehwag, Edoardo Debenedetti, Nicolas Flammarion, Mung Chiang, Prateek Mittal, and Matthias Hein, "Robustbench: a standardized adversarial robustness benchmark," in *Thirty-fifth Conference on Neural Information Processing Systems Datasets and Benchmarks Track*, 2021. 19

[5] TensorFlow, "Tensorflow datasets." 19

[6] AgriPredict, "Agripredict disease-classification." 19

[7] Jun-Yan Zhu, Taesung Park, Phillip Isola, and Alexei A. Efros, "Unpaired image-to-image translation using cycle-consistent adversarial networks," 2020. 19

[8] Bolei Zhou, Agata Lapedriza, Aditya Khosla, Aude Oliva, and Antonio Torralba, "Places: A 10 million image database for scene recognition," *IEEE Transactions on Pattern Analysis and Machine Intelligence*, 2017. 19, 22

[9] Kai Han, Yunhe Wang, Qi Tian, Jianyuan Guo, Chunjing Xu, and Chang Xu, "Ghostnet: More features from cheap operations," 2020. 19, 26

[10] Ping Chao, Chao-Yang Kao, Yu-Shan Ruan, Chien-Hsiang Huang, and Youn-Long Lin, "Hardnet: A low memory traffic network," 2019. 19

[11] Alex Krizhevsky, Ilya Sutskever, and Geoffrey E Hinton, "Imagenet classification with deep convolutional neural networks," in *Advances in Neural Information Processing Systems* (F. Pereira, C. J. C. Burges, L. Bottou, and K. Q. Weinberger, eds.), vol. 25, Curran Associates, Inc., 2012. 19, 31

[12] Gao Huang, Zhuang Liu, Laurens van der Maaten, and Kilian Q. Weinberger, "Densely connected convolutional networks," 2018. 19, 20, 26, 31

[13] Raunak Dey and Yi Hong, "Compnet: Complementary segmentation network for brain mri extraction," 2018. 19, 20

[14] Christian Szegedy, Wei Liu, Yangqing Jia, Pierre Sermanet, Scott Reed, Dragomir Anguelov, Dumitru Erhan, Vincent Vanhoucke, and Andrew Rabinovich, "Going deeper with convolutions," 2014. 20, 31

[15] Nicolas Carion, Francisco Massa, Gabriel Synnaeve, Nicolas Usunier, Alexander Kirillov, and Sergey Zagoruyko, "End-to-end object detection with transformers," 2020. 20

[16] Mark Sandler, Andrew Howard, Menglong Zhu, Andrey Zhmoginov, and Liang-Chieh Chen, "Mobilenetv2: Inverted residuals and linear bottlenecks," 2019. 20, 27, 31

[17] Christian Szegedy, Vincent Vanhoucke, Sergey Ioffe, Jonathon Shlens, and Zbigniew Wojna, "Rethinking the inception architecture for computer vision," 2015. 20, 30, 31

[18] Kaiming He, Xiangyu Zhang, Shaoqing Ren, and Jian Sun, "Deep residual learning for image recognition," 2015. 20, 21, 28, 29, 31

[19] Karen Simonyan and Andrew Zisserman, "Very deep convolutional networks for large-scale image recognition," 2015. 21, 31

[20] Johannes Hofmanninger, Forian Prayer, Jeanny Pan, Sebastian Röhrich, Helmut Prosch, and Georg Langs, "Automatic lung segmentation in routine imaging is primarily a data diversity problem, not a methodology problem," *European Radiology Experimental*, vol. 4, Aug. 2020. 21

[21] Zhiqiang Shen and Marios Savvides, "Meal v2: Boosting vanilla resnet-50 to 80 21

[22] Justin Johnson, Alexandre Alahi, and Li Fei-Fei, "Perceptual losses for real-time style transfer and super-resolution," 2016. 21, 22

[23] René Ranftl, Katrin Lasinger, David Hafner, Konrad Schindler, and Vladlen Koltun, "Towards robust monocular depth estimation: Mixing datasets for zero-shot cross-dataset transfer," 2020. 21

[24] Mingxing Tan and Quoc V. Le, "Efficientnet: Rethinking model scaling for convolutional neural networks," 2020. 21, 26, 29, 30

[25] Shah Nawaz, Alessandro Calefati, Moreno Caraffini, Nicola Landro, and Ignazio Gallo, "Are these birds similar: Learning branched networks for fine-grained representations," in *2019 International Conference on Image and Vision Computing New Zealand (IVCNZ)*, pp. 1–5, 2019. 21

[26] Rasmus Rothe, Radu Timofte, and Luc Van Gool, "Dex: Deep expectation of apparent age from a single image," in *2015 IEEE International Conference on Computer Vision Workshop (ICCVW)*, pp. 252–257, 2015. 21, 22

[27] Emad Barsoum, Cha Zhang, Cristian Canton Ferrer, and Zhengyou Zhang, "Training deep networks for facial expression recognition with crowd-sourced label distribution," 2016. 21

[28] Wei Liu, Dragomir Anguelov, Dumitru Erhan, Christian Szegedy, Scott Reed, Cheng-Yang Fu, and Alexander C. Berg, "Ssd: Single shot multibox detector," 2016. 21

[29] Andrew G. Howard, Menglong Zhu, Bo Chen, Dmitry Kalenichenko, Weijun Wang, Tobias Weyand, Marco Andreetto, and Hartwig Adam, "Mobilenets: Efficient convolutional neural networks for mobile vision applications," 2017. 21

[30] Wenzhe Shi, Jose Caballero, Ferenc Huszár, Johannes Totz, Andrew P. Aitken, Rob Bishop, Daniel Rueckert, and Zehan Wang, "Real-time single image and video super-resolution using an efficient sub-pixel convolutional neural network," 2016. 22

[31] Tsung-Yi Lin, Priya Goyal, Ross Girshick, Kaiming He, and Piotr Dollár, "Focal loss for dense object detection," 2018. 22

[32] Linzaer, "Ultra-lightweight face detection model." https://github.com/Linzaer/Ultra-Light-Fast-Generic-Face-Detector-1MB, 2019. 22

[33] Joseph Redmon and Ali Farhadi, "Yolov3: An incremental improvement," 2018. 22

[34] Tero Karras, Timo Aila, Samuli Laine, and Jaakko Lehtinen, "Progressive growing of gans for improved quality, stability, and variation," 2018. 22

[35] Joseph Redmon and Ali Farhadi, "Yolo9000: Better, faster, stronger," 2016. 22

[36] Alexey Bochkovskiy, Chien-Yao Wang, and Hong-Yuan Mark Liao, "Yolov4: Optimal speed and accuracy of object detection," 2020. 22

[37] Matthew D Zeiler and Rob Fergus, "Visualizing and understanding convolutional networks," 2013. 22

[38] Hang Zhang, Chongruo Wu, Zhongyue Zhang, Yi Zhu, Haibin Lin, Zhi Zhang, Yue Sun, Tong He, Jonas Mueller, R. Manmatha, Mu Li, and Alexander Smola, "Resnest: Split-attention networks," 2020. 22, 23, 28, 29

[39] Jiankang Deng, Jia Guo, Niannan Xue, and Stefanos Zafeiriou, "Arcface: Additive angular margin loss for deep face recognition," 2019. 22

[40] Panqu Wang, Pengfei Chen, Ye Yuan, Ding Liu, Zehua Huang, Xiaodi Hou, and Garrison Cottrell, "Understanding convolution for semantic segmentation," 2018. 22

[41] Xintao Wang, Liangbin Xie, Chao Dong, and Ying Shan, "Real-esrgan: Training real-world blind super-resolution with pure synthetic data," 2021. 22, 23

[42] Hirokatsu Kataoka, Kazushige Okayasu, Asato Matsumoto, Eisuke Yamagata, Ryosuke Yamada, Nakamasa Inoue, Akio Nakamura, and Yutaka Satoh, "Pre-training without natural images," 2020. 22

[43] Sravanti Addepalli, Samyak Jain, Gaurang Sriramanan, Shivangi Khare, and Venkatesh Babu Radhakrishnan, "Towards achieving adversarial robustness beyond perceptual limits," in *ICML 2021 Workshop on Adversarial Machine Learning*, 2021. 22

[44] Maksym Andriushchenko and Nicolas Flammarion, "Understanding and improving fast adversarial training," 2020. 22

[45] Maximilian Augustin, Alexander Meinke, and Matthias Hein, "Adversarial robustness on in- and out-distribution improves explainability," 2020. 23

[46] Yair Carmon, Aditi Raghunathan, Ludwig Schmidt, Percy Liang, and John C. Duchi, "Unlabeled data improves adversarial robustness," 2019. 23

[47] Jinghui Chen, Yu Cheng, Zhe Gan, Quanquan Gu, and Jingjing Liu, "Efficient robust training via backward smoothing," 2020. 23

[48] Tianlong Chen, Sijia Liu, Shiyu Chang, Yu Cheng, Lisa Amini, and Zhangyang Wang, "Adversarial robustness: From self-supervised pre-training to fine-tuning," 2020. 23

[49] Jiequan Cui, Shu Liu, Liwei Wang, and Jiaya Jia, "Learnable boundary guided adversarial training," 2021. 23

[50] James Diffenderfer, Brian R. Bartoldson, Shreya Chaganti, Jize Zhang, and Bhavya Kailkhura, "A winning hand: Compressing deep networks can improve out-of-distribution robustness," 2021. 23

[51] Gavin Weiguang Ding, Yash Sharma, Kry Yik Chau Lui, and Ruitong Huang, "Mma training: Direct input space margin maximization through adversarial training," in *International Conference on Learning Representations*, 2020. 23

[52] Logan Engstrom, Andrew Ilyas, Hadi Salman, Shibani Santurkar, and Dimitris Tsipras, "Robustness (python library)," 2019. 23

[53] Robert Geirhos, Patricia Rubisch, Claudio Michaelis, Matthias Bethge, Felix A. Wichmann, and Wieland Brendel, "Imagenet-trained cnns are biased towards texture; increasing shape bias improves accuracy and robustness," 2019. 23

[54] Sven Gowal, Chongli Qin, Jonathan Uesato, Timothy Mann, and Pushmeet Kohli, "Uncovering the limits of adversarial training against norm-bounded adversarial examples," 2021. 23, 24

[55] Dan Hendrycks, Kimin Lee, and Mantas Mazeika, "Using pre-training can improve model robustness and uncertainty," 2019. 23

[56] Dan Hendrycks, Norman Mu, Ekin D. Cubuk, Barret Zoph, Justin Gilmer, and Balaji Lakshminarayanan, "Augmix: A simple data processing method to improve robustness and uncertainty," 2020. 23, 24

[57] Dan Hendrycks, Steven Basart, Norman Mu, Saurav Kadavath, Frank Wang, Evan Dorundo, Rahul Desai, Tyler Zhu, Samyak Parajuli, Mike Guo, Dawn Song, Jacob Steinhardt, and Justin Gilmer, "The many faces of robustness: A critical analysis of out-of-distribution generalization," 2021. 24

[58] Lang Huang, Chao Zhang, and Hongyang Zhang, "Self-adaptive training: beyond empirical risk minimization," 2020. 24

[59] Klim Kireev, Maksym Andriushchenko, and Nicolas Flammarion, "On the effectiveness of adversarial training against common corruptions," 2021. 24

[60] Hanxun Huang, Yisen Wang, Sarah Monazam Erfani, Quanquan Gu, James Bailey, and Xingjun Ma, "Exploring architectural ingredients of adversarially robust deep neural networks," 2021. 24

[61] Rahul Rade and Seyed-Mohsen Moosavi-Dezfooli, "Helper-based adversarial training: Reducing excessive margin to achieve a better accuracy vs. robustness trade-off," in *ICML 2021 Workshop on Adversarial Machine Learning*, 2021. 24

[62] Tianyu Pang, Xiao Yang, Yinpeng Dong, Kun Xu, Jun Zhu, and Hang Su, "Boosting adversarial training with hypersphere embedding," 2020. 24

[63] Sylvestre-Alvise Rebuffi, Sven Gowal, Dan A. Calian, Florian Stimberg, Olivia Wiles, and Timothy Mann, "Fixing data augmentation to improve adversarial robustness," 2021. 24, 25

[64] Leslie Rice, Eric Wong, and J. Zico Kolter, "Overfitting in adversarially robust deep learning," 2020. 25

[65] Jérôme Rony, Luiz G. Hafemann, Luiz S. Oliveira, Ismail Ben Ayed, Robert Sabourin, and Eric Granger, "Decoupling direction and norm for efficient gradient-based l2 adversarial attacks and defenses," 2019. 25

[66] Hadi Salman, Andrew Ilyas, Logan Engstrom, Ashish Kapoor, and Aleksander Madry, "Do adversarially robust imagenet models transfer better?," 2020. 25

[67] Vikash Sehwag, Shiqi Wang, Prateek Mittal, and Suman Jana, "Hydra: Pruning adversarially robust neural networks," 2020. 25

[68] Vikash Sehwag, Saeed Mahloujifar, Tinashe Handina, Sihui Dai, Chong Xiang, Mung Chiang, and Prateek Mittal, "Robust learning meets generative models: Can proxy distributions improve adversarial robustness?," 2021. 25

[69] Chawin Sitawarin, Supriyo Chakraborty, and David Wagner, "Sat: Improving adversarial training via curriculum-based loss smoothing," 2021. 25

[70] Kaustubh Sridhar, Oleg Sokolsky, Insup Lee, and James Weimer, "Improving neural network robustness via persistency of excitation," 2021. 25

[71] Yisen Wang, Difan Zou, Jinfeng Yi, James Bailey, Xingjun Ma, and Quanquan Gu, "Improving adversarial robustness requires revisiting misclassified examples," in *International Conference on Learning Representations*, 2020. 25

[72] Eric Wong, Leslie Rice, and J. Zico Kolter, "Fast is better than free: Revisiting adversarial training," 2020. 25

[73] Dongxian Wu, Shu tao Xia, and Yisen Wang, "Adversarial weight perturbation helps robust generalization," 2020. 25

[74] Hongyang Zhang, Yaodong Yu, Jiantao Jiao, Eric P. Xing, Laurent El Ghaoui, and Michael I. Jordan, "Theoretically principled trade-off between robustness and accuracy," 2019. 25

[75] Dinghuai Zhang, Tianyuan Zhang, Yiping Lu, Zhanxing Zhu, and Bin Dong, "You only propagate once: Accelerating adversarial training via maximal principle," 2019. 25

[76] Jingfeng Zhang, Jianing Zhu, Gang Niu, Bo Han, Masashi Sugiyama, and Mohan Kankanhalli, "Geometry-aware instance-reweighted adversarial training," 2021. 25

[77] Jingfeng Zhang, Xilie Xu, Bo Han, Gang Niu, Lizhen Cui, Masashi Sugiyama, and Mohan Kankanhalli, "Attacks which do not kill training make adversarial learning stronger," 2020. 25

[78] M. Salvaris, M. Kaznady, V. Paunic, I. Karmanov, A. Bhatia, W.H. Tok, and S. Chikkerur, "Deepseismic: a deep learning library for seismic interpretation," vol. 2020, no. 1, pp. 1–5, 2020. 25

[79] Nikita Misiura, "starnet." https://github.com/nekitmm/starnet, 2018. 25

[80] Han Zhang, Tao Xu, Hongsheng Li, Shaoting Zhang, Xiaogang Wang, Xiaolei Huang, and Dimitris Metaxas, "Stackgan++: Realistic image synthesis with stacked generative adversarial networks," 2018. 25

[81] Tero Karras, Samuli Laine, and Timo Aila, "A style-based generator architecture for generative adversarial networks," 2019. 25, 26

[82] Alexey Kurakin, Ian Goodfellow, and Samy Bengio, "Adversarial machine learning at scale," 2017. 26

[83] My Kieu, Andrew D. Bagdanov, Marco Bertini, and Alberto Del Bimbo, "Domain adaptation for privacy-preserving pedestrian detection in thermal imagery.," in *ICIAP (2)*, pp. 203–213, 2019. 26

[84] Weijian Xu, Yifan Xu, Tyler Chang, and Zhuowen Tu, "Co-scale conv-attentional image transformers," 2021. 26

[85] Chien-Yao Wang, Hong-Yuan Mark Liao, I-Hau Yeh, Yueh-Hua Wu, Ping-Yang Chen, and Jun-Wei Hsieh, "Cspnet: A new backbone that can enhance learning capability of cnn," 2019. 26

[86] Fisher Yu, Dequan Wang, Evan Shelhamer, and Trevor Darrell, "Deep layer aggregation," 2019. 26

[87] Shang-Hua Gao, Ming-Ming Cheng, Kai Zhao, Xin-Yu Zhang, Ming-Hsuan Yang, and Philip Torr, "Res2net: A new multi-scale backbone architecture," 2021. 26, 28

[88] Yunpeng Chen, Jianan Li, Huaxin Xiao, Xiaojie Jin, Shuicheng Yan, and Jiashi Feng, "Dual path networks," 2017. 26

[89] Qilong Wang, Banggu Wu, Pengfei Zhu, Peihua Li, Wangmeng Zuo, and Qinghua Hu, "Eca-net: Efficient channel attention for deep convolutional neural networks," 2020. 26

[90] Suyog Gupta and Mingxing Tan, "Efficientnet-edgetpu: Creating accelerator-optimized neural networks with automl," Aug 2019. 26, 30

[91] Youngwan Lee, Joong won Hwang, Sangrok Lee, Yuseok Bae, and Jongyoul Park, "An energy and gpu-computation efficient backbone network for real-time object detection," 2019. 26

[92] Mingxing Tan and Quoc V. Le, "Efficientnetv2: Smaller models and faster training," 2021. 26, 30

[93] Bichen Wu, Xiaoliang Dai, Peizhao Zhang, Yanghan Wang, Fei Sun, Yiming Wu, Yuandong Tian, Peter Vajda, Yangqing Jia, and Kurt Keutzer, "Fbnet: Hardware-aware efficient convnet design via differentiable neural architecture search," 2019. 26

[94] Christian Szegedy, Sergey Ioffe, Vincent Vanhoucke, and Alex Alemi, "Inception-v4, inception-resnet and the impact of residual connections on learning," 2016. 26, 27

[95] Ming Lin, Hesen Chen, Xiuyu Sun, Qi Qian, Hao Li, and Rong Jin, "Neural architecture design for gpu-efficient networks," 2020. 26

[96] Jian Guo, He He, Tong He, Leonard Lausen, Mu Li, Haibin Lin, Xingjian Shi, Chenguang Wang, Junyuan Xie, Sheng Zha, Aston Zhang, Hang Zhang, Zhi Zhang, Zhongyue Zhang, Shuai Zheng, and Yi Zhu, "Gluoncv and gluonnlp: Deep learning in computer vision and natural language processing," *Journal of Machine Learning Research*, vol. 21, no. 23, pp. 1–7, 2020. 27

[97] Niv Nayman, Yonathan Aflalo, Asaf Noy, and Lihi Zelnik-Manor, "Hardcore-nas: Hard constrained differentiable neural architecture search," 2021. 27

[98] Jingdong Wang, Ke Sun, Tianheng Cheng, Borui Jiang, Chaorui Deng, Yang Zhao, Dong Liu, Yadong Mu, Mingkui Tan, Xinggang Wang, Wenyu Liu, and Bin Xiao, "Deep high-resolution representation learning for visual recognition," 2020. 27

[99] Jie Hu, Li Shen, Samuel Albanie, Gang Sun, and Enhua Wu, "Squeeze-and-excitation networks," 2019. 27, 29

[100] Mingxing Tan and Quoc V. Le, "Mixconv: Mixed depthwise convolutional kernels," 2019. 27, 30

[101] Mingxing Tan, Bo Chen, Ruoming Pang, Vijay Vasudevan, Mark Sandler, Andrew Howard, and Quoc V. Le, "Mnasnet: Platform-aware neural architecture search for mobile," 2019. 27, 29, 31

[102] Andrew Howard, Mark Sandler, Grace Chu, Liang-Chieh Chen, Bo Chen, Mingxing Tan, Weijun Wang, Yukun Zhu, Ruoming Pang, Vijay Vasudevan, Quoc V. Le, and Hartwig Adam, "Searching for mobilenetv3," 2019. 27, 28, 30

[103] Byeongho Heo, Sangdoo Yun, Dongyoon Han, Sanghyuk Chun, Junsuk Choe, and Seong Joon Oh, "Rethinking spatial dimensions of vision transformers," 2021. 28

[104] Nathan Silberman and Sergio Guadarrama, "Tensorflow-slim image classification model library." https://github.com/tensorflow/models/tree/master/research/slim, 2016. 28

[105] Ilija Radosavovic, Raj Prateek Kosaraju, Ross Girshick, Kaiming He, and Piotr Dollár, "Designing network design spaces," 2020. 28

[106] Chenxi Liu, Barret Zoph, Maxim Neumann, Jonathon Shlens, Wei Hua, Li-Jia Li, Li Fei-Fei, Alan Yuille, Jonathan Huang, and Kevin Murphy, "Progressive neural architecture search," 2018. 28

[107] Xiaohan Ding, Xiangyu Zhang, Ningning Ma, Jungong Han, Guiguang Ding, and Jian Sun, "Repvgg: Making vgg-style convnets great again," 2021. 28

[108] Irwan Bello, William Fedus, Xianzhi Du, Ekin D. Cubuk, Aravind Srinivas, Tsung-Yi Lin, Jonathon Shlens, and Barret Zoph, "Revisiting resnets: Improved training and scaling strategies," 2021. 29

[109] Saining Xie, Ross Girshick, Piotr Dollár, Zhuowen Tu, and Kaiming He, "Aggregated residual transformations for deep neural networks," 2017. 29, 31

[110] Dongyoon Han, Sangdoo Yun, Byeongho Heo, and YoungJoon Yoo, "Rethinking channel dimensions for efficient model design," 2021. 29

[111] Dushyant Mehta, Oleksandr Sotnychenko, Franziska Mueller, Weipeng Xu, Mohamed Elgharib, Pascal Fua, Hans-Peter Seidel, Helge Rhodin, Gerard Pons-Moll, and Christian Theobalt, "Xnect: Real-time multi-person 3d motion capture with a single rgb camera," 2020. 29

[112] Xiang Li, Wenhai Wang, Xiaolin Hu, and Jian Yang, "Selective kernel networks," 2019. 29

[113] Dimitrios Stamoulis, Ruizhou Ding, Di Wang, Dimitrios Lymberopoulos, Bodhi Priyantha, Jie Liu, and Diana Marculescu, "Single-path nas: Designing hardware-efficient convnets in less than 4 hours," 2019. 29

[114] I. Zeki Yalniz, Hervé Jégou, Kan Chen, Manohar Paluri, and Dhruv Mahajan, "Billion-scale semi-supervised learning for image classification," 2019. 29

[115] Cihang Xie, Mingxing Tan, Boqing Gong, Jiang Wang, Alan Yuille, and Quoc V. Le, "Adversarial examples improve image recognition," 2020. 29, 30

[116] Qizhe Xie, Minh-Thang Luong, Eduard Hovy, and Quoc V. Le, "Self-training with noisy student improves imagenet classification," 2020. 29, 30

[117] François Chollet, "Xception: Deep learning with depthwise separable convolutions," 2017. 30

[118] Zhengsu Chen, Lingxi Xie, Jianwei Niu, Xuefeng Liu, Longhui Wei, and Qi Tian, "Visformer: The vision-friendly transformer," 2021. 30

[119] Kai Han, Yunhe Wang, Qiulin Zhang, Wei Zhang, Chunjing Xu, and Tong Zhang, "Model rubik's cube: Twisting resolution, depth and width for tinynets," 2020. 30

[120] Sergey Zagoruyko and Nikos Komodakis, "Wide residual networks," 2017. 30, 31, 32

[121] Xiangxiang Chu, Zhi Tian, Yuqing Wang, Bo Zhang, Haibing Ren, Xiaolin Wei, Huaxia Xia, and Chunhua Shen, "Twins: Revisiting the design of spatial attention in vision transformers," 2021. 30, 31

[122] Changqian Yu, Jingbo Wang, Chao Peng, Changxin Gao, Gang Yu, and Nong Sang, "Learning a discriminative feature network for semantic segmentation," 2018. 31

[123] Hengshuang Zhao, Jianping Shi, Xiaojuan Qi, Xiaogang Wang, and Jiaya Jia, "Pyramid scene parsing network," 2017. 31

[124] Ningning Ma, Xiangyu Zhang, Hai-Tao Zheng, and Jian Sun, "Shufflenet v2: Practical guidelines for efficient cnn architecture design," 2018. 31

[125] Forrest N. Iandola, Song Han, Matthew W. Moskewicz, Khalid Ashraf, William J. Dally, and Kurt Keutzer, "Squeezenet: Alexnet-level accuracy with 50x fewer parameters and ¡0.5mb model size," 2016. 31

[126] Joseph Paul Cohen, Mohammad Hashir, Rupert Brooks, and Hadrien Bertrand, "On the limits of cross-domain generalization in automated x-ray prediction," 2020. 31, 32

[127] Olaf Ronneberger, Philipp Fischer, and Thomas Brox, "U-net: Convolutional networks for biomedical image segmentation," 2015. 32

[128] Ultralytics, "Yolov5." https://github.com/ultralytics/yolov5, 2020. 32